

Department of Precision and Microsystems Engineering

Stage inaccuracy compensation on sub-micrometer flatness measurement

Sjoerd Zillen

Report no : 2023.010
Coach : Dr. ir. J.F.C. van Gorp (ASML)
Professor : Dr. N. Bhattacharya
Specialisation : Mechatronic system design
Type of report : Thesis
Date : 02/02/2023

Abstract

Flatness is an important surface tolerance requirement during the manufacturing of a part of an ASML machine. Flatness can be measured by either measuring the variation in height of the surface in one measurement (a plane-wise measurement) or by measuring the height on multiple xy-coordinates on this surface (point-wise measurement). Point-wise distance measurement sensors tend to have small physical dimensions, while having good specifications on resolution perpendicular to the measured surface. During a separate research, a gap is found in performing a point-wise flatness measurement while accounting for undesired stage deviations. The stage deviations are in the order of micrometers, while the sensor accuracy is in the order of nanometers. The performance of a point-wise flatness measurement is therefore in a negative sense dominated by the stage inaccuracies rather than sensor performance. During this research the gap is filled by designing, building and testing a feasibility demonstrator which uses reference sensors to account for stage inaccuracies. By performing a live correction with either 1 or 3 reference sensors, the stage inaccuracy (in z, Rx and Ry) can be compensated for. The measured stage wobble for this specific setup is $3.2 \mu\text{m}$, which is reduced to $0.13 \mu\text{m}$ when using three reference sensors. The method of using reference sensors for flatness measurements is shown to work, mainly when using 3 reference sensors.

Contents

1	Introduction	3
1.1	Problem statement	3
1.2	Literature summary	3
1.3	Research assignment	6
1.4	Layout of the thesis	6
2	Measurement systems	7
2.1	System 1: No reference sensors	7
2.2	System 2: One sensor for z referencing	8
2.3	System 3: Three sensors for z Rx Ry referencing	9
3	Design of experiments	10
3.1	Introduction	10
3.2	Test setup	11
3.2.1	Sensors	11
3.2.2	Optical flat	12
3.2.3	Definition of coordinate system and sensor numbering	12
3.3	Sensor tests	13
3.3.1	Test the repeatability of the sensor	13
3.4	Thermal tests	14
3.4.1	Static thermal effects of the setup	14
3.4.2	Dynamic thermal effects of the setup	15
3.4.3	Conclusions	16
3.5	Optical flat measuring	17
3.5.1	Measuring with one stage and the main sensor	17
3.5.2	Determine measurement pitch	18
3.5.3	Measuring with one stage, the main sensor and one reference sensor	19
3.5.4	Measuring with one stage, the main sensor and three reference sensor sensors	20
3.5.5	Measuring with two stages and the main sensor	23
3.5.6	Distinction of random and reproducible stage inaccuracies with two stages	24
3.5.7	Measuring with two stages, the main sensor and one reference sensor	26
3.5.8	Measuring with two stages, the main sensor and three reference sensors	27
3.6	Experimental optimization	29
3.6.1	3D printed parts	29
3.6.2	Test the sensor on receiving a value	30
3.6.3	Sensors validation	31
4	Discussion and recommendations	33
4.1	Discussion and recommendations for improvement of performance	33
4.1.1	Thermal effects	33
4.1.2	Determine measurement pitch	33
4.1.3	Sensor errors	34
4.1.4	Random and reproducible xy-stage inaccuracies	34
4.1.5	Addition of reference sensors	35
4.1.6	Setup limitations	36
5	Conclusion and outlook	37
5.1	Conclusion	37
5.2	Outlook	38
5.2.1	Different sensor placement	38
5.2.2	Calibration method in combination with reference sensor	38
A	Literature report	39

Chapter 1: Introduction

1.1 Problem statement

ASML is well known for being a worldwide innovation leader in the semiconductor industry. ASML provides the lithography machines, which provide an essential step in the mass production of computer chips. Since the worldwide demand for computer chips keeps increasing, ASML is pushing boundaries to keep up with the demand. The demand for chips with more transistors per area, while being attractive in price, keeps increasing. The production machines of ASML must be pushed to the limit in order to keep up with the demand. Pushing the limits goes hand in hand with increasing the complexity of the machines. Such complex machines consist of thousands of parts. For such a machine to work, it is of importance that every part within the machine cooperates and fits together seamlessly. In order for all the parts of the machine to cooperate and fit together, the parts must be manufactured within specified tolerances. Examples of such tolerances on parts are dimensions, fits, stiffness, roughness and flatness. The last is of importance for this research. Flatness is defined as the maximum distance between two parallel planes on either side of the surface. All points of the surface must lie between the two parallel planes to meet the flatness requirements. Flatness must not be confused with parallelism, figure 1 shows the difference between flatness and parallelism clearly. The research done in this report is about verifying a method for measuring flatness during the production process of a part of an ASML machine.

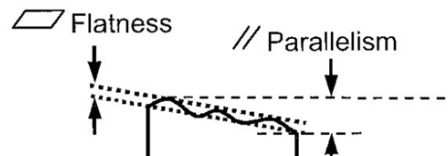


Figure 1: Flatness tolerance zone [1]

1.2 Literature summary

Prior to this thesis, a separate yet related, literature research is done. This section gives an summary of the literature research. The full literature study can be found in appendix A, which is only available for the committee members of the graduation project due to intellectual property. The goal of the literature study was to find answers on the following questions:

- Which measurement methods are invented to determine flatness?
- What is the typical performance of these methods?

The questions stated above are answered extensively in the literature research. To get an overview of all flatness measurement methods, a tree diagram is made. This tree diagram is shown in Figure 2. Flatness can be measure by performing a plane measurement, or by combining multiple points which are measured on an xy plane. The three diagram contains both point-wise and plane-wise flatness measurements, which will be explained further in section 1.3. The tree diagram is split into two main branches, contact measurement methods and non-contact measurement methods. The contact measurement methods consist of coordinate measurement machines and scanning probe microscopes. Additional information on contact measurement methods can be found in section 3.3 of appendix A. The non-contact measurement branch consists of scanning probe microscopes (section 3.5.2 of appendix A), capacitive (section 3.5.3 of appendix A), electron (section 3.5.4 of appendix A) and optical (section 3.4 of appendix A). As can be seen, the optical section is the most extensive section since these are the most commonly used method found in literature on flatness measurement methods.

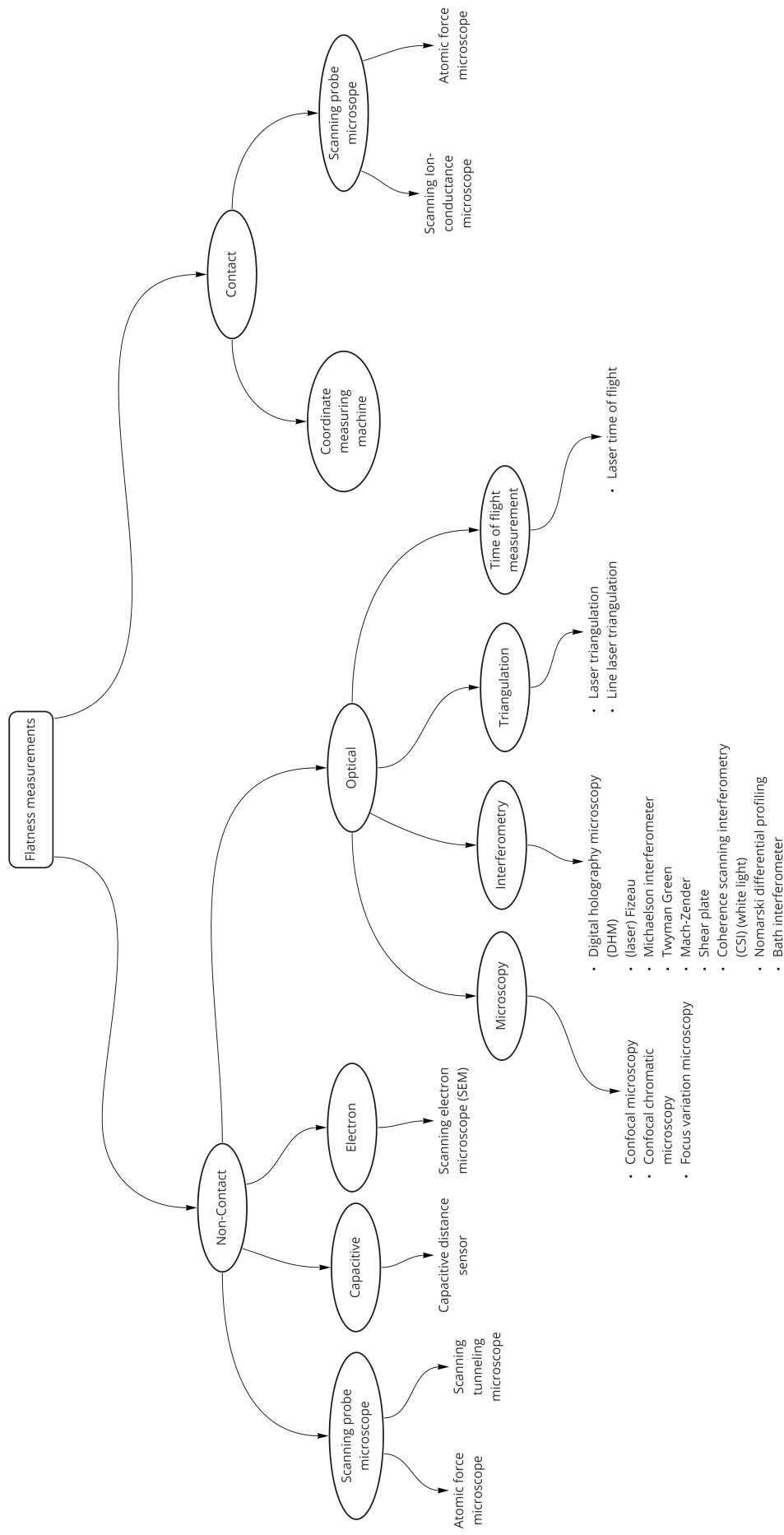


Figure 2: Tree diagram of measurement methods

The tree diagram consists of measurement methods of which some do and some do not match the needs from the initial problem. In order to get an overview of the typical performance of the measurement methods, an overview table is created. The full overview table can be found in the literature study, which can be found in appendix A. Down below in table 1 an overview is shown with suitable methods. The top row contains the criteria, the other rows are the measurement methods which meet the requirements. Both the Fizeau and Twyman Green interferometer are methods with a high resolution perpendicular to the surface while having a small spacial resolution. The Fizeau interferometer tends to have better fringe contrast, which comes at a higher price. The downside of these methods are the dimensions. The confocal chromatic microscope and the point-wise interferometer have a good resolution with a relatively small spot-size while being small in dimensions. These methods are the point-wise measurement type, thus errors due to grid scanning will be induced in the measurements, which will be elaborated on in subsection 1.3. The laser triangulation sensor is a point-wise measurement method which has a lower resolution perpendicular to the surface in comparison with the other methods and has a bigger spot-size.

Measurement method	Resolution perpendicular to surface	Spot size	Dimensions	Measurement time	Measurement type
(laser) Fizeau interferometer	1.5nm	4 μ m	121 x 97 x 57mm	1 min	Plane
Twyman green interferometer	1.5nm	4 μ m	121 x 97 x 57mm	1 min	Plane
Confocal chromatic microscopy	3nm	3 μ m	\varnothing 12mm x 60mm	12 min	Point
Point-wise Coherence scanning (white light) interferometer	1nm ***	10 μ m ***	\varnothing 10mm x 55mm***	12 min	Point
Laser triangulation	30nm	50 μ m	100x75x30 mm	12 min	Point

Table 1: Suitable measurement methods

1.3 Research assignment

As can be seen on table 1 in subsection 1.2, two measurement types are being distinguished. The measurement type can either be a plane measurement or a point-wise measurement. Although point-wise measurement methods have small dimensions, while having good specifications on resolution perpendicular to the surface, this resolution is not reached on flatness measurements. To deduct flatness out of a point-wise measurement, multiple measurements on different xy-locations must be done on the sample under test. Out of these different measurements on different locations, flatness can be determined. Since either the sample or the sensor must be moved in the xy-plane, an xy-stage must be used. Unfortunately, a stage introduces additional deviations. Figure 3 shows the definition of these undesired deviations. Deviation in x,y and yaw (R_z) only influence the location which is measured on the xy plane, so these degrees of freedom do not introduce a noticeable error in flatness. Since flatness is relevant for this project, the other three degrees of freedom which are causing errors in the flatness measurement are of importance. These three degrees of freedom are flatness (deviation in z), pitch (deviation in R_x) and roll (deviation in R_y). Pitch and roll cause undesired deviations, since these deviations cause error in flatness. This error is created due to an arm between the pivot point and the measurement point. The arm times the angle results in an error in z. The total stage inaccuracy is a combination of z, R_x and R_y .

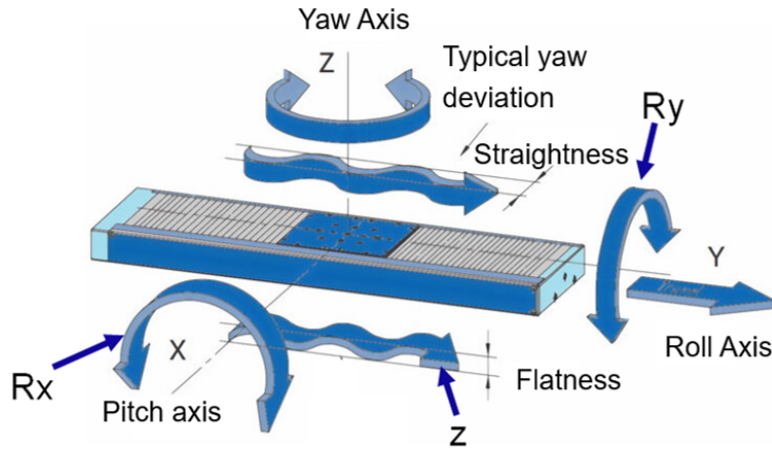


Figure 3: Stage undesired deviation definition [2]

During the literature research, a gap in the literature is found on performing a set of point-wise measurements to deduct flatness from, while accounting for stage inaccuracies. The stage flatness is in the order of micrometers, while the sensor accuracy is in the order of nanometers. The performance of a pointwise flatness measurement is therefore in a negative sense dominated by the stage inaccuracies rather than sensor performances. During this research, the gap is filled by designing, building and testing a feasibility demonstrator which performs a point-wise flatness measurement while accounting for stage inaccuracies. The goal of this feasibility demonstrator is to determine flatness of a sample with better accuracy than stage inaccuracies. The feasibility demonstrator will measure the sample simultaneously with the stage deviations, such that the flatness of the sample can be measured while accounting for stage deviations. This will be explained and elaborated on further in section 2. During this research the following research questions are answered

- What is the order of magnitude of the different stage inaccuracies and what is the influence in z measurements?
- What are the improvements in z measurements by calibrating the setup or adding either one or three reference sensors?
- What are the next physical limiting factors in accuracy after implementing the reference sensors?

1.4 Layout of the thesis

First, several point-wise measurement systems are shown in section 2. After an explanation of the measurement systems is given, section 3 will go into the design of experiment. This section will describe all experiments required to verify the measurement system. Results will be discussed, conclusions will be drawn and recommendations will be given in section 4.

Chapter 2: Measurement systems

As described in subsection 1.2, several measurement methods are suitable to determine flatness. Section 1.3 describes that the performance of a point-wise measurement is negatively dominated by stage inaccuracies rather than sensor performance. This section describes several flatness measuring systems on performing point-wise measurements to measure flatness while accounting for stage inaccuracies. The working principle of each system is the same, a reference plane with a known (and low) flatness is attached to the linear stage which is able to move in the xy-plane. The distance perpendicular to the moving stage (z) is measured point-wise by measuring the reference plane. The reference plane is an optical flat, which is a precisely manufactured piece of glass with a specified flatness. Since the flatness of the optical flat is several orders lower than the stage inaccuracies, stage inaccuracies are dominant when measuring the optical flat. As described in section 1.3, three degrees of freedom of the stage cause inaccuracies in z -distance measurements. These degrees of freedom are flatness (deviation in z), pitch (deviation in R_x) and roll (deviation in R_y). If all three degrees of freedom of the optical flat are measured, the stage inaccuracies are effectively measured. As a sample is placed on the optical flat, the optical flat and the sample can be measured simultaneously. Both the stage inaccuracies and the sample are point-wise measured. The actual sample flatness can be extracted from the data by deducting the stage inaccuracies data from the sample measurement data.

The stage has inaccuracies are expected to be partly random and partly reproducible. Random inaccuracies are not reproducible, which makes it difficult to be compensated for. Reproducible inaccuracies can be compensated by first measuring the optical flat to map the stage inaccuracies. Once the inaccuracies are mapped, a sample can be measured and the stage inaccuracy data can be used to compensate. This unfortunately does not work for random measurement inaccuracies. The measurement principle which is described in this research is to account for both random inaccuracies and reproducible inaccuracies, since it measured the stage inaccuracies simultaneously with the sample. The research is done to validate the measurement principle rather than measuring a sample. In order to validate the measurement system, this chapter goes into three systems on compensating for stage inaccuracies by measuring with multiple sensors. Subsection 2.1 explains the system without reference sensors, subsection 2.2 explains the system with one reference sensor and subsection 2.3 explains the system with three reference sensors.

2.1 System 1: No reference sensors

Figure 4 shows a sketch of measurement system 1 to measure a sample without reference sensors. This measurement system consists of one sensor, an optical flat and two stages. The sensor is denoted as main sensor and measures the distance z from the sensor to the sample. In a practical case, a sample would be measured by the sensor. As explained above, no sample is measured during this research. The goal of this research is on feasibility of the measurement system, thus the system shown in figure 5 is used during this research. Instead of a sample with an unknown flatness, an optical flat with a known flatness is used. To determine point-wise flatness, multiple distance measurements must be done on the optical flat on different locations. To be able to measure multiple points in the xy- plane, two linear stages are combined together. The stages available to use at ASML are the Thorlabs NRT150/M. The stage inaccuracy in z is not specified by the manufacturer, but is expected to be in the order of $20 \mu\text{m}$ over the whole length of the stage. The inaccuracy is expected to be both random and reproducible. It is unknown whether random or reproducible inaccuracies dominate the stage inaccuracies. The measurement will be a combination of z , R_x and R_y inaccuracies. Since only one sensor is used, different stage inaccuracies (z , R_x and R_y) cannot be distinguished.

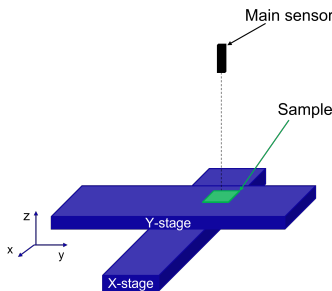


Figure 4: Sketch of practical system 1: No reference sensors (with sample)

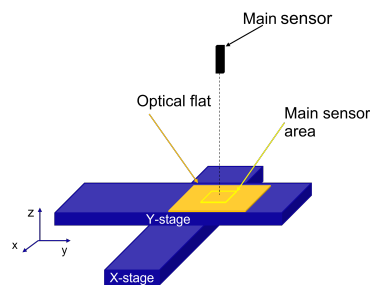


Figure 5: Sketch of research system 1: No reference sensors (without sample)

2.2 System 2: One sensor for z referencing

Figure 6 shows a sketch of measurement system 2. One sensor is used to measure the sample, denoted as main sensor. The second sensor, denoted as reference sensor, is added to measure the optical flat. As the optical flat is measured, stage inaccuracies are measured simultaneously with the sample. As explained in the introduction, no sample will be measured during the research. The measurement system as shown in figure 7 will be used during this research. The main sensor area is the area on the optical flat where an sample would be placed.

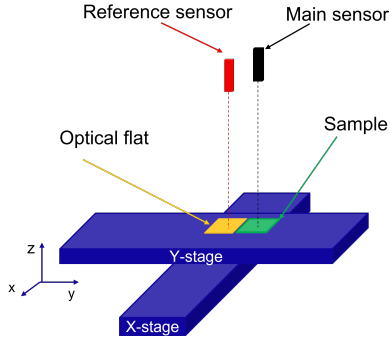


Figure 6: Sketch of practical system 2: One sensor for z referencing (with sample)

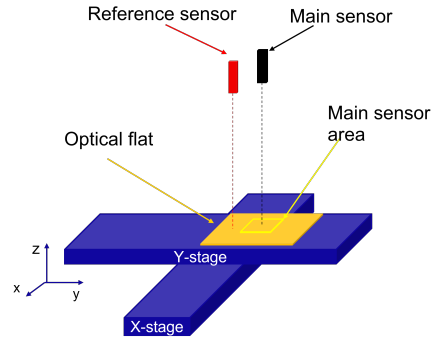


Figure 7: Sketch of research system 2: One sensor for z referencing

Since one reference sensor is used, stage inaccuracies will be measured and accounted for. Since one reference sensor is used, a distinguish between stage inaccuracies flatness (z), pitch (R_x) or roll (R_y) cannot be made. The reference sensor is not on the same location as the sample sensor, so introduced stage inaccuracies on either R_x or R_y result in an inaccuracy in z on the main sensor. A calculation is done to predict the effect of R_x and R_y inaccuracies on the measurement of the optical flat. The stage has a specified pitch inaccuracy of $140 \mu\text{rad}$. The roll inaccuracy is not specified, thus is also expected to be $140 \mu\text{rad}$. Two stages are attached onto each other, the total pitch/roll inaccuracy is then $280 \mu\text{rad}$. The distance between the reference sensor and the main sensor is estimated to be 0.05m . A sketch of the situation is shown in figure 8. These values are used to calculate z : $z = \alpha * L = 280 \mu\text{rad} * 0.05\text{m} = 14 \mu\text{m}$.

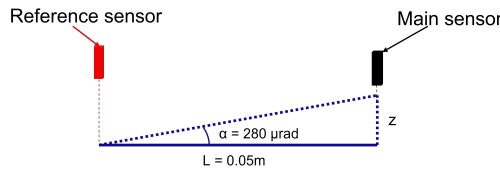


Figure 8: Calculation of z variation due to R_x

2.3 System 3: Three sensors for z Rx Ry referencing

The system uses a sample, an optical flat and four sensors in total and is shown on figure 9. One main sensor is used to measure the sample and three reference sensors are used to measure three degrees of freedom of the optical flat and thus the stage inaccuracies. The sample is placed on top of the optical flat, such that the optical flat is located around the sample. Since the optical flat is around the sample, no extrapolation is required on the reference sensors. As mentioned before, three degrees of freedom cause stage inaccuracies, which are z, Rx and Ry. As the optical flat is measured pointwise, the main sensor measures the sample and the three reference sensors measure the optical flat simultaneously. Since all three degrees of freedom of stage inaccuracies are measured, the stage inaccuracy for every individual measurement point is measured. The stage inaccuracy measurement can then be deducted from the signal of the main sensor, after which the stage deviation is removed from the flatness measurement. Since no sample is used during the research, the optical flat will be measured with four sensors in total. This configuration is shown in figure 10. All degrees of freedom of the stage are measured with the three reference sensors, so during this research the main sensor is mainly used to validate the measurement system.

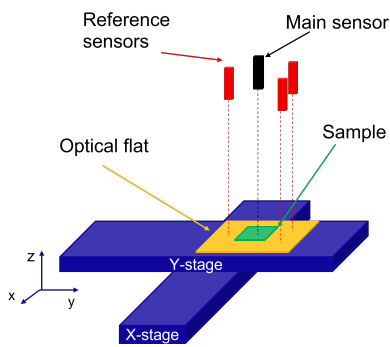


Figure 9: Sketch of practical system 3: Three sensors for z referencing (with sample)

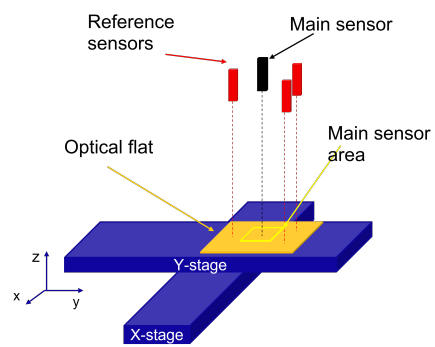


Figure 10: Sketch of research system 3: Three sensors for z Rx Ry referencing

Chapter 3: Design of experiments

3.1 Introduction

In order to test the measurement systems which are described in chapter 2, a design of experiments is made. This chapter will go into the design of experiments, by going through a testplan. The tests in this testplan are in order of increasing complexity, with milestones during the tests. Figure 11 gives an overview of all the tests done in this chapter. The setup will be explained briefly, after which the testplan execution will be described. First the sensors are tested in section 3.3, which leads to the first milestone. As the milestone is achieved, the tests beneath it can be executed. The second tests are on the thermal effects of the setup, which is elaborated on in section 3.4. As the thermal effects are known, measurements of the optical flat on the stages can be done. The set of tests on measuring the optical flat is described in section 3.5.

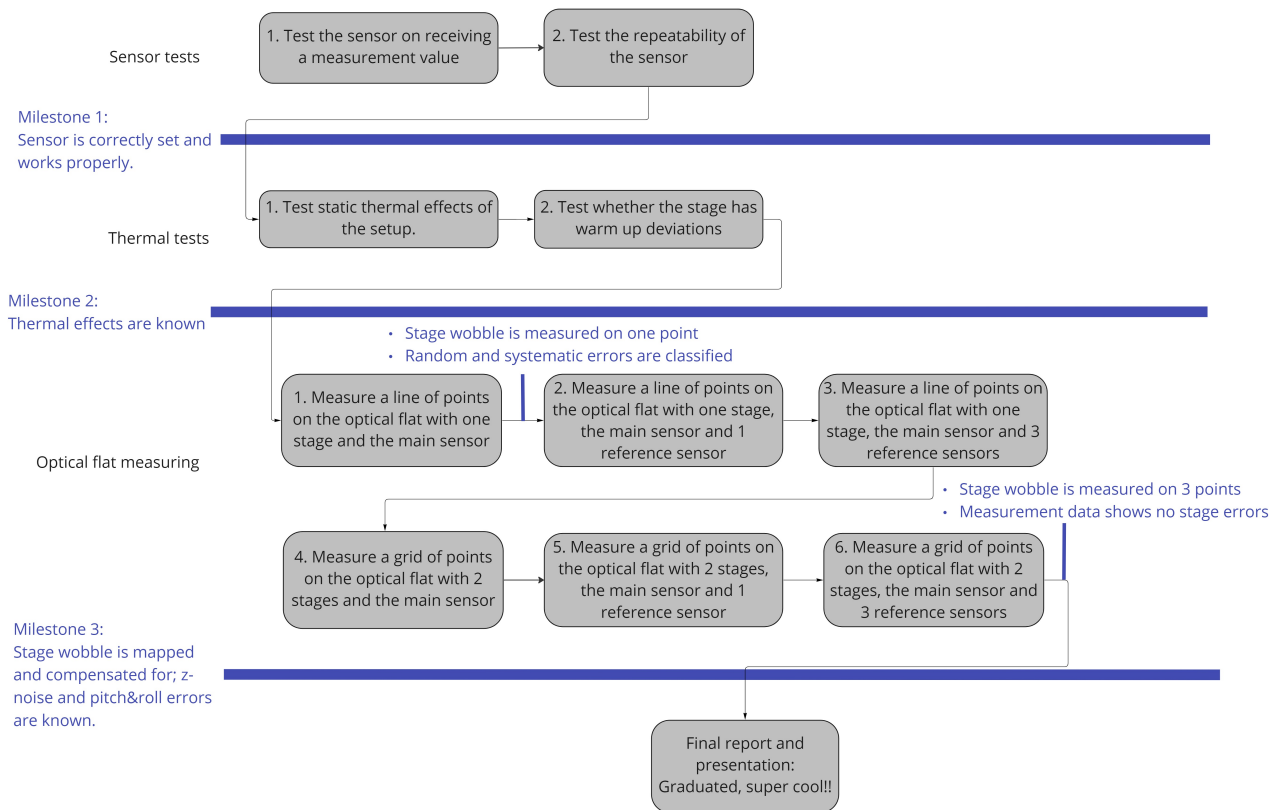


Figure 11: Test diagram

3.2 Test setup

The CAD model of the setup on which the tests are executed is shown in figure 12. The setup consists of a breadboard (5) on which a frame of aluminum profiles (1) is attached. The sensors are attached on an aluminum sensor holder (2). There are three capacitive sensors (6) which are the reference sensors to measure the optical flat (3) and one confocal sensor (7) which measures the main sensor area. The optical flat is attached to the two stages (8) by using an optical flat holder (4). Temperature is expected to be a dominant factor in the setup therefore six temperature sensors are located throughout the system. The locations of these temperature sensors will be described during the tests in this chapter. To control the stages and read out the temperature and sensors, a computer and sensor control boxes are used, which are not added to the figure. The working principle of the setup is explained in chapter 2.

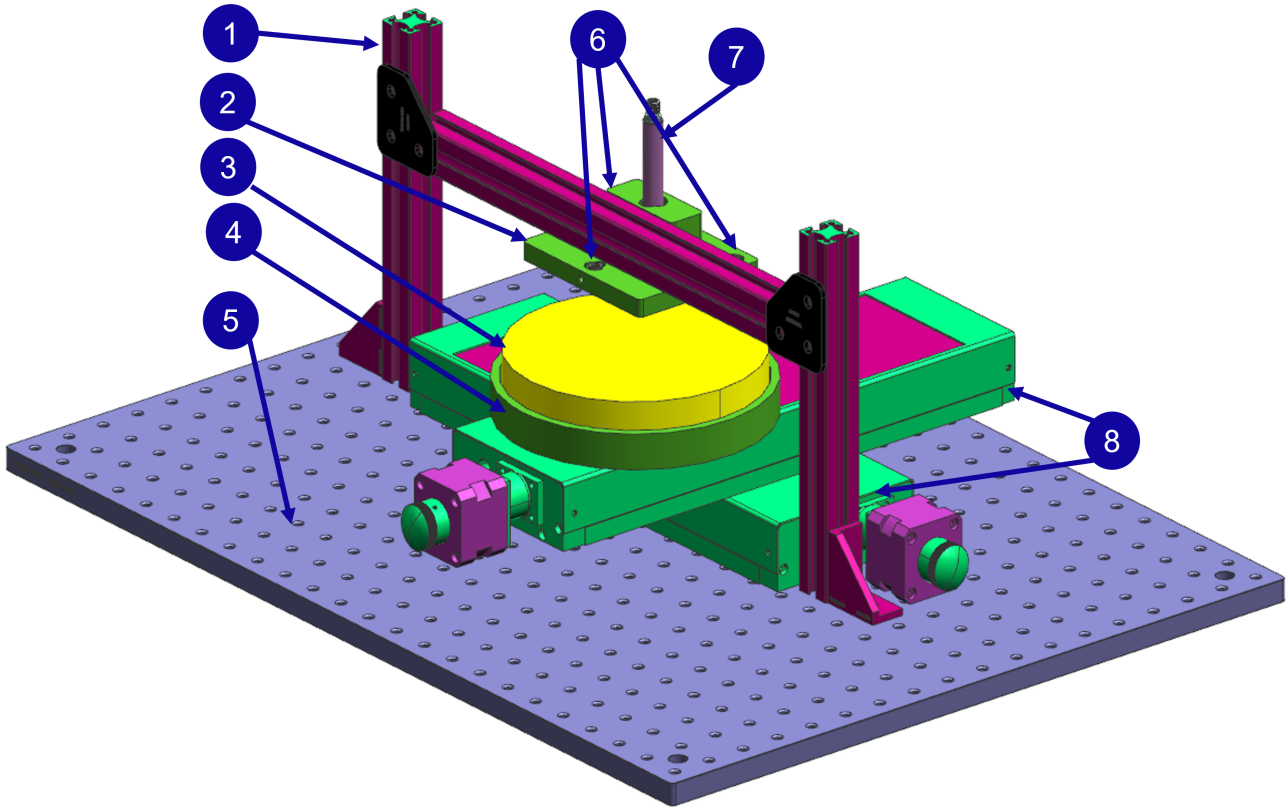


Figure 12: Test setup CAD model

3.2.1 Sensors

main sensor The main sensor is a confocal sensor of micro epsilon. The working principle of the sensor is described in appendix A . The confocal sensor is chosen due to the small spot-size of $6\mu\text{m}$ and high resolution of 24nm . The sensor works well on reflective surfaces. The specific type of sensor is the 2407-0,8 which has a measurement range of $800\mu\text{m}$.

Reference sensor The reference sensors are the sensors which measure the optical flat which is mounted on the stage. The reference sensors are three identical capacitive sensors. In the literature report in appendix A, the capacitive sensor did not seem within the requirements due to the large spotsizes. Since the spotsizes matters less for the reference sensors, capacitive sensors are an ideal choice due to high resolutions while being small in dimensions. The capacitive sensors which are used in the setup are the micro epsilon CS05 sensors, have a measurement range of $500\mu\text{m}$ with a resolution of 0.375nm . The measurement spot of the sensor is $\text{Ø}3.9\text{mm}$.

3.2.2 Optical flat

As described previously, an optical flat is used as reference plane for the setup. An optical flat is an precisely manufactured piece of glass with a known flatness. The optical flat is a gold coated optical flat with a diameter of 152.4mm, manufactured by Edmund optics. The gold coating is required for the capacitive sensors to work properly. The optical flat is specified to have a flatness of $\frac{\lambda}{10} = \frac{632.8nm}{10} = 63.28nm$. This flatness is 1-2 orders of magnitude lower than the expected stage wobble, thus will not dominate the stage deviation which is to be measured.

3.2.3 Definition of coordinate system and sensor numbering

In figure 13, a top view of the setup is shown with introduced coordinate systems. Two coordinate systems are introduced. One coordinate system is the movement of the stage, namely xyz. Stage coordinates are the input for the system to move, with origin at the location of the optical flat on the homed xy- stage. The second coordinate system is for the location of the sensors with respect to each other, namely uvw. The origin is the point on the xy-plane where the confocal sensor is placed. The uvw coordinate system is introduced for calculation purposes, which will be addressed later. Figure 14 shows the numbering of the sensors. The three reference sensors (r_1, r_2, r_3) are the capacitive sensors, the main sensor (m_1) is the confocal sensor. The reference sensors are placed in a circular pattern with an angle of 120° .

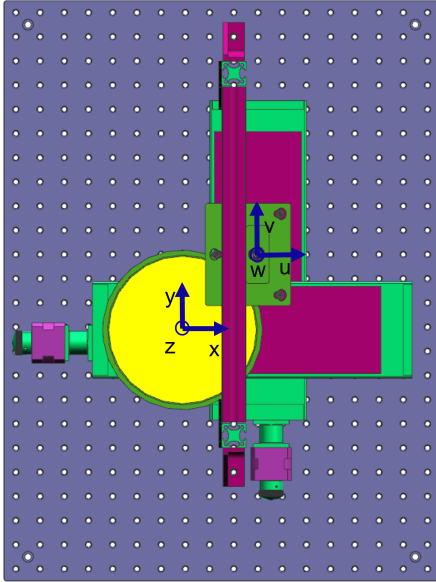


Figure 13: Top view of test setup with introduced coordinate system

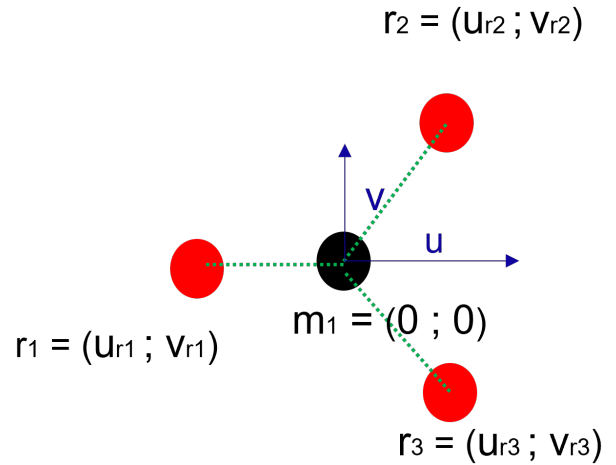


Figure 14: Sensor placement and naming

3.3 Sensor tests

This section is about tests related to the performance of the sensors. The sensors first had to be installed and aligned, which can be found in chapter 3.6 (experimental optimization). The repeatability of the sensors is tested in subsection 3.3.1.

3.3.1 Test the repeatability of the sensor

Repeatability refers to how reliable a sensor can repeat the same measurement. The conditions of the measurement must not change while measuring repeatability. Repeatability is an important specification of a sensor, as it gives a value on the noise which the value has during measurements. The manufacturer does not specify repeatability of these sensors, so it will be measured in this section.

Expectations Repeatability is not specified by the manufacturer, but linearity and sensitivity errors are. For the capacitive sensor the linearity error is $< \pm 0.05\%$ of the measurement range and the sensitivity is $< \pm 0.1\%$ of the measurement range. This would result in a maximum error of $\pm 0.5 \mu\text{m} + \pm 0.25 \mu\text{m}$, which is $< \pm 0.75 \mu\text{m}$ in total. Linearity error is constant over a small measurement range. Due to this, it is expected to have a repeatability of approximately $\pm 0.25 \mu\text{m}$ for the capacitive sensor.

For the confocal sensor, only a linearity error is specified, which is $< \pm 0.025\%$ of the measurement range, which leads to $< \pm 0.2 \mu\text{m}$. Since the linearity error is constant over a small measurement range, it is expected that the sensor has little to no errors in measurements.

Implementation To test repeatability, it is of importance to perform multiple measurement while keeping the variables the same. To test the repeatability, the cable of the sensor cable is pulled in and out the control box. After 5 seconds a measurement takes place and is stored.

Results First the confocal sensor is tested, the result is shown down below in figure 15. The x-axis shows the measurements, the y axis shows the deviation in Z in μm . To analyze the data, the standard deviation is calculated. The standard deviation SD is calculated by $SD = \sqrt{\frac{\sum (x_i - \bar{x})^2}{(N-1)}}$. Whereby x_i is an individual measurement value, \bar{x} is the average of the measurement values and N is the amount of measurements done. The 3SD of the repeatability of the confocal sensor is $\pm 0.0723 \mu\text{m}$, Which means that 99.73% of the measurements is within $\pm 0.0723 \mu\text{m}$ as deviation when taking 3SD. As for the confocal sensor only a linearity error was mentioned, it was expected to have low errors as measured.

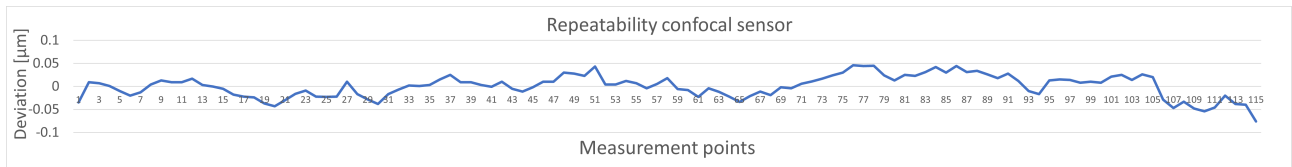


Figure 15: Repeatability test confocal sensor

Secondly, the capacitive sensors are tested. The results are shown in table 2 and figure 16.

	Capacitive sensor 1 [μm]	Capacitive sensor 2 [μm]	Capacitive sensor 3 [μm]
3SD	± 0.049	± 0.080	± 0.079

Table 2: Standard deviation capacitive sensors

The repeatability of the sensors are better then expected.

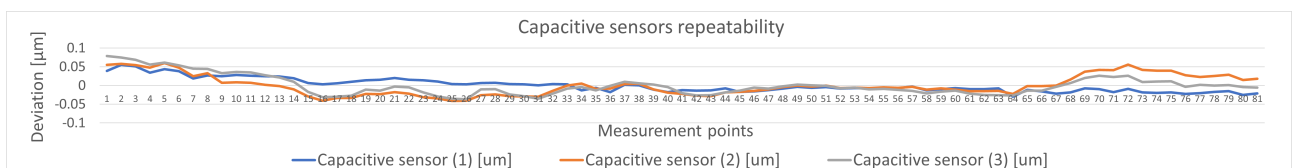


Figure 16: Repeatability test capacitive sensor

3.4 Thermal tests

Thermal effects are expected to have influence on the measurements done on the system. The goal of this chapter is get the order of magnitude of change in sensor readings due to thermal effects. The insights gained during this section are used to determine the impact of temperature changes during later tests. Firstly in section 3.4.1, temperature changes in the environment are related to sensor readings. This is done by measuring the temperature and sensor readings simultaneously, while keeping the stages of the setup stationary. Secondly in section 3.4.2, heating of the stage due to movement of the stage is related to sensor readings over time. A repeated stage movement is done while measuring both the temperature on several spots on the setup and the sensor readings. The required time to get to steady state is measured during this test.

3.4.1 Static thermal effects of the setup

Temperature deviation is expected have effect on the measurement data. This test is done to verify the effect of temperature deviations on the sensor readings. The goal of this test is to get the order of magnitude of the introduced measurement errors due to temperature deviations of the environment. Sensor readings are done on an interval of 10 seconds over a 48h period, while temperature is measured simultaneously.

Expected The setup is located in a cleanroom which has a temperature deviation rating of ± 0.5 K. Temperature deviations are expected to have a direct relation with sensor readings. There are two thermal effects which occur. The first being the temperature variation of the sensor and its electronics, the second being the thermal expansion of the whole setup. The deviation of the sensor readings due to thermal effects are not specified by the sensor manufacturer, but is expected to be small in comparison with the thermal expansion of the whole setup. Unfortunately, thermal expansion of the setup will occur, thus these effects cannot be separated and will be measured together. Since the sensor have a resolution in the nanometer range, it is expected that the order of magnitude of the introduced errors due to thermal effects can be measured by the sensors.

Implementation The sample and reference sensors are monitoring the distance of the sensor with respect to the optical flat and measurement data is stored every ten seconds. Temperature of the setup and environment are measured simultaneously. In order to measure the temperature, an Arduino and 6 negative temperature coefficient (NTC) probes are ordered and assembled. Multiple temperature probes are used to monitor the temperature on several spots on the setup and the environment simultaneously. Figure 17 and figure 18 shows the setup with the six temperature probes (blue cables). The probes are attached by using kapton tape and thermal paste. The probes with label 1, 2, 5 and 6 are located on the stage. Probe 3 measures the temperature of the aluminum extruded profile, which is expected to measure similar temperatures to the measured temperature of the environment (probe 4). Probe 4 is expected to have the most noise, since the thermal mass is lower and the probe could be effected more by air flowing against the probe. Temperature probe 3 will be used to relate the distance sensor signal with the environmental temperature in the cleanroom. Once the two tests are explained and results are shown, conclusions will be finally drawn in subsection 3.4.3

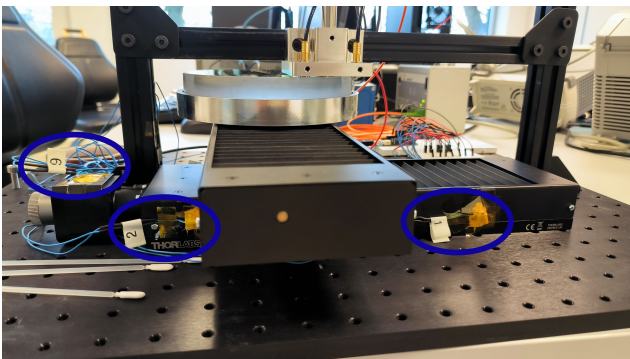


Figure 17: Temperature sensors location



Figure 18: Temperature sensors location other side

Results Figure 19 shows the measurement data over a period of 48 hours. The x-axis shows the time of the measurements, the y axis shows the deviation in sensor readings in μm , and the deviation in temperature in K. The average of each individual sensor is subtracted from the individual sensor, such that all sensor data can be compared evenly. There is a clear relation between the sensor readings and the temperature readings. The temperature is more stable during night times, since there are less factors for noise (such as people moving in and out the cleanroom). As the temperature increases, the sensor readings increases. The three capacitive sensors react in sync, while the confocal sensor deviates from capacitive signals on temperature deviation. This can be clearly seen from 21:00 till 08:00 on day 2, indicated with the blue square in figure 19. The deviation between the capacitive sensors and the confocal sensor is roughly 50nm. This stability is only after the setup had a redesign, which is described in section 3.6.1.

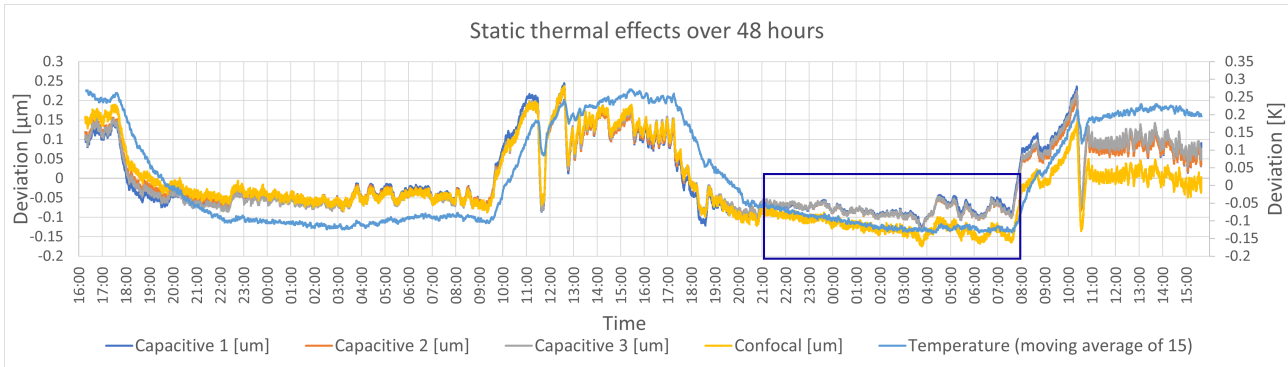


Figure 19: Static thermal effects over 48 hours

3.4.2 Dynamic thermal effects of the setup

The linear stages will heat up during movement due to friction and due to electrical dissipation. This test is done to relate the thermal effects of the stage to the sensor measurements. As the thermal effects are known, the stages can be warmed up until steady state is reached for further tests. Alternatively, the time of usage of the stage is short such that the warm-up effects are not noticeable.

Expected As the stage heats up, expansion of materials will occur due to thermal effects. This expansion is expected to have effect on sensor readings. Since materials tend to expand with an increase in temperature, the sensor readings are expected to measure a lower absolute distance once the stage heats up. The effect of stage-warm up will only be noticeable in measurement system 1 and partly in 2 (of chapter 2), since system 3 will fully compensate for deviations due to stage inaccuracies. The measurement value is expected to increase at first and to be stable once the temperature of the stage is at steady state.

Implementation The stage will move back and forth over the range of the optical flat with increments of 1mm and the absolute distance of the sensors with respect to the optical flat will be measured on each step. Since the effective measurement range over the optical flat is 100mm, 100 steps will be made over the optical flat. The effective measurement range are in between $x = 35\text{mm}$ to $x = 135\text{mm}$. As it is unknown when the stage will reach steady state so, the stage will move back and forth 40 times in a row over this distance. Since the stage moved back and forth for 40 times over a range of 100mm with increments of 1mm, 8000 points are measured. It takes roughly 2 seconds to reach the next point and measure, so the measurement takes place over a period of roughly 4,5 hours. The stage is expected to have reached steady state after this period. As mentioned in subsection 3.4.1, several temperature probes are attached to the system. The stepper motor will generate heat, which will conduct through the frame of the stage. To monitor the heat distribution of the stage, several temperature probes are attached. By measuring the temperature in combination with the distance sensor readings, the time to steady state can be determined. The distance sensor readings are expected to deviate at first, and then converge once the stage has reached thermal steady state.

Results As the measurement is performed 40 times back and forth, each measurement location is measured 80 times. Each measurement point of each sensor in the middle of the optical flat ($x = 85\text{mm}$) is plotted over time in figure 20. The average of each sensor is subtracted from the measurement, to make it a relative measurement. The corresponding axis with the deviations in μm is the left y-axis is the left axis. The temperature of the temperature probe number 2 is added and has a second y-axis which is the temperature in K. Temperature probe 2 is located on the frame of the stage near the stepper motor. The temperature deviation is averaged to reduce noise in the signal. Looking at the temperature, the temperature increases the most significant in the first 1.5 hours, after which the temperature is stable for 1 hour until roughly 2:30. After this point, the environmental temperature drops 0.05 K. Looking at the measurement data of the sensors, the temperature of the stage seem to have minor impact on the measurement data.

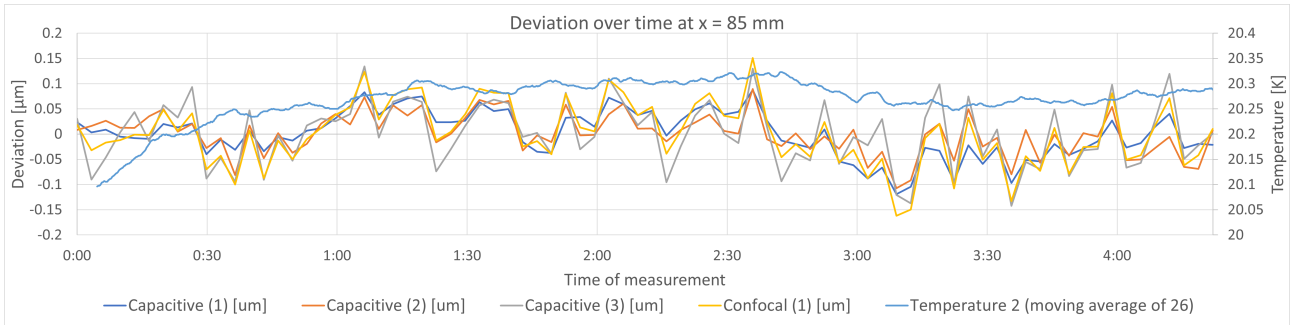


Figure 20: Deviation over time due to stage warm-up on the middle of the optical flat

3.4.3 Conclusions

Temperature deviations have influence on the measurement data. The static thermal effects shows a difference of roughly 300nm during deviations of temperature in the cleanroom. The principle of the setup is by comparing the relative sensor measurements with each other. It is therefore of importance that all the sensors behave in the same relative matter when temperature changes. The individual sensors deviate with a value of roughly 50nm with respect to each other, which contributes to the error of the total system during flatness measurements when using reference sensor. In general, the quicker the measurements, the less chance on deviation in temperature, thus the better. The dynamic thermal effects of the stage have minor impact on the distance measurements in comparison with the the static (environmental) thermal changes. Moving the stage till thermal steady state is reached is therefore not required for further tests.

3.5 Optical flat measuring

The section is about measuring the optical flat with the distance sensors. First the optical flat is measured with one sensor and the separation between random and reproducible stage inaccuracies is determined. With the measurement data, a minimum required pitch between measurement points is determined. Once a pitch is determined, the optical flat is measured with either one, two or four sensors. First the optical flat is measured with one stage, after which the same tests are done with two stages. By adding more sensors, each system described in chapter 2 is tested.

3.5.1 Measuring with one stage and the main sensor

As described in subsection 3.1, first the stage inaccuracies are measured with one stage and one sensor. The goal of this test is to classify the contribution of random and reproducible inaccuracies of the stage. The distinction of random and reproducible inaccuracies is of importance, since reproducible inaccuracies can be compensated when measured once. The measurement principle which is described in this research is to account for both random inaccuracies and reproducible inaccuracies, since it measured the stage inaccuracies simultaneously with the sample.

Expected The sensors are in the nanometer range and the optical flat has a flatness which is several orders lower than the expected stage inaccuracy, so stage inaccuracies will be measured when measuring the optical flat. The manufacturer of the stage only specifies a tilt error of $140\mu\text{rad}$, while inaccuracy in z is not specified. Since it is not specified, it is unknown what the deviation in z of the stage will be although it is estimated to be in the order of $20\mu\text{m}$. It is expected that the stage has inaccuracies which are partly random and partly reproducible.

Implementation To measure the stage inaccuracies, a line of points is measured on the optical flat. The linear stage will move the optical flat over a range of 100 mm, while the main sensor measures the absolute distance of the sensor with respect to the optical flat. After the absolute distance is measured by the sensor on the optical flat, the average will be subtracted to convert the absolute measurements in relative measurements. The relative measurement distances will be plotted over the range of the stage to visualize the inaccuracies in z of the stage. The plot shows the combination of random and reproducible inaccuracies. Multiple measurements will be done, after which the contribution of random and reproducible inaccuracies of the stage can be split. By subtracting two separate measurements, the random error is separated from the reproducible error.

Results Down below in figure 21, the deviation of the sensor is plotted over the location of the stage, thus the optical flat. The difference between the maximum and the minimum deviation is roughly $13\mu\text{m}$.

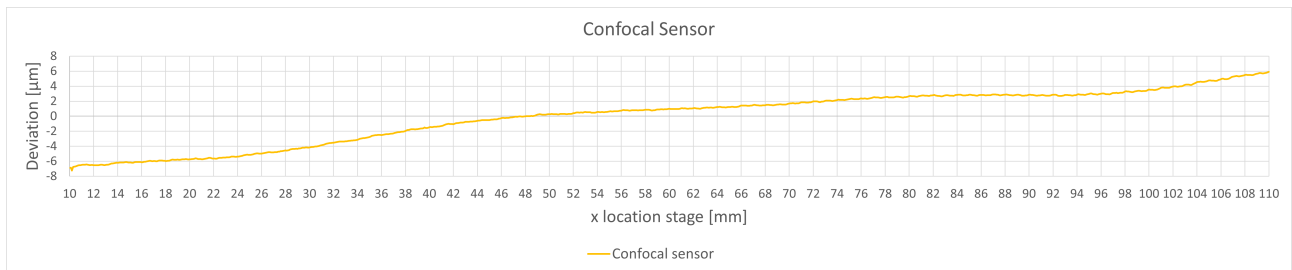


Figure 21: Stage deviation by main sensor

A slope is observed in the measurement of the optical flat. This could either be due to stage inaccuracies or due to the top surface of the optical flat not moving perpendicular to the sensor, which can be verified once more sensors are introduced. To remove this slope a linear fit is done on the measurement, which is then subtracted from the measurement data. The results of the measurements minus the linear slope can be seen in figure 22. The graph shows the difference between the maximum and the minimum in deviation is roughly $3\mu\text{m}$ over this range of the stage, which is significantly lower in comparison with the difference in variation of figure 21.

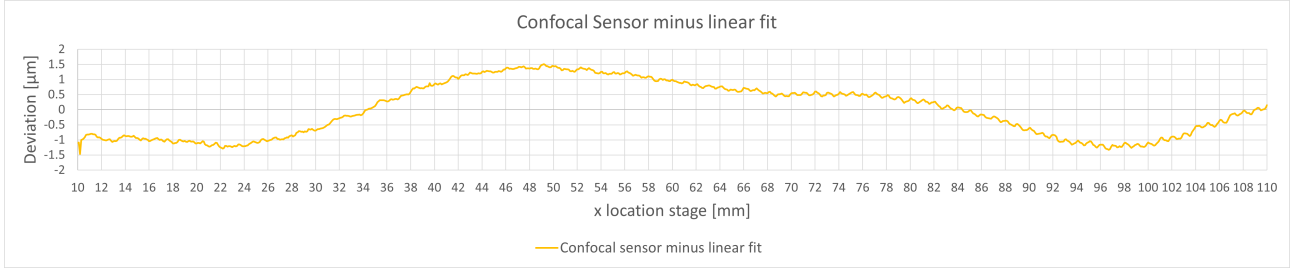


Figure 22: Stage deviation minus linear fit

In order to distinguish the random inaccuracies from the reproducible inaccuracies, a second measurement is done and subtracted from the first measurement data. The random stage inaccuracies are shown in figure 23. The random stage inaccuracies are determined to be $0.4 \mu\text{m}$ after analyzing the data.

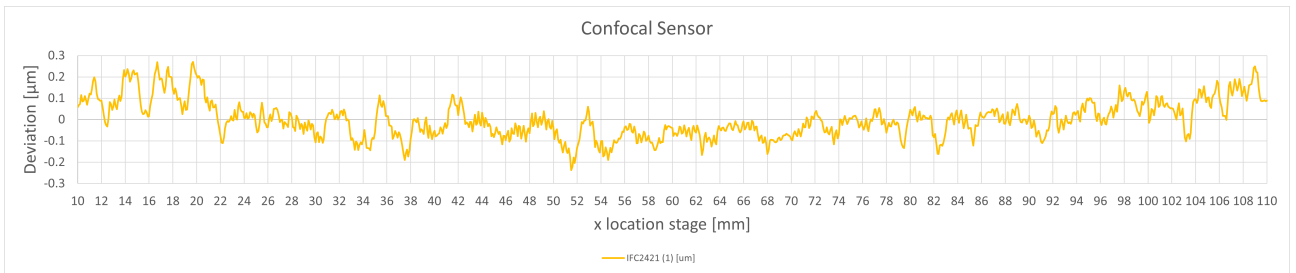


Figure 23: Random stage deviations

3.5.2 Determine measurement pitch

As described in subsection 3.4.3, the measurement time is preferred to be as low as possible. The measurement time is decreased by increasing the stage speed, decreasing the required measurement time per measurement point or decreasing the amount of measurement points. The measurement time is reduced most effectively by reducing the amount of measurement points. As the amount of measurement points on the same measurement line/area decreases, the pitch between the measurement points increases. Obviously, the less measurement points, the less data is acquired. In this subsection the maximum pitch (and thus minimum amount of measurement points) while a sufficient amount measurement points is determined.

Expected Depending on the spatial frequency of the deviation in z of the stage, the minimum pitch between measurements can be determined. As the pitch increases, the amount of measurement points decreases. To obtain the required information, a sufficient amount of measurement points must be taken over the measurement range of the stage. According to Figliola [3], the minimum required measurement frequency to preserve both frequency and amplitude of the signal is described. The measurement frequency must be 10 times the highest frequency which is to be measured. A schematic overview of the introduced error is shown in figure 24 and 25. Since the measurement is a pointwise measurement, the measurement frequency is determined by the spatial measurement period, thus stepsize. The stepsize (period of the measurement) must be 10 times smaller than the period of the stage inaccuracy

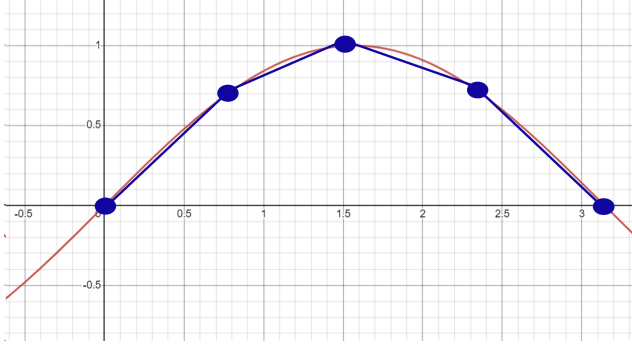


Figure 24: fine measurement pitch

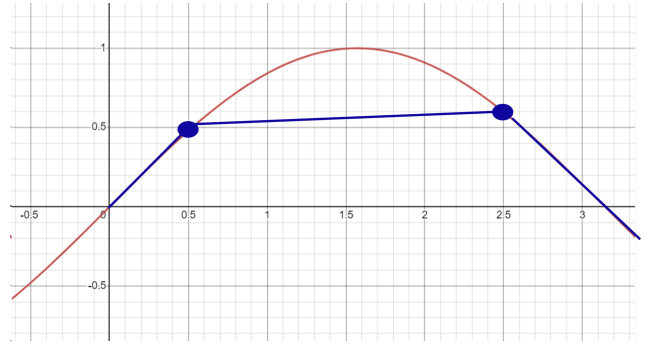


Figure 25: course measurement pitch

Implementation The measurement data from figure 22 from subsection 3.5.1 can be used to determine the measurement pitch. As described above, the minimum measurement frequency (which determines the pitch) must be 10 times greater than the highest frequency which is to be measured.

Results Figure 22 shows a high frequent deviation over the whole measurement range with a period of 1 mm. The stage is moved by the use of a screw spindle, which has a pitch of 1 mm. Due to the spindle, an error is introduced. The error is reproducible and has an amplitude of roughly 50 nm, which leads to an additional error of 100 nm (which will be compensated anyhow when using three reference sensors). Since the measurement frequency must be 10 times higher than the frequency of the signal, the required measurement pitch would be 100 μm . The deviation with the second highest frequency is the deviation with the period of 50 mm till 74 mm, which is a period of 24 mm and thus results in a measurement pitch of 2.4 mm. Required measurement time scales linearly with the amount of measurement points, so the measurement time for a line is 24 times longer if a measurement pitch of 100 μm is used compared to a pitch of 2.4 mm. Due to this, it is chosen not to measure the error introduces by the spindle. To be on the safe side, a measurement pitch of 2 mm is used for further tests.

3.5.3 Measuring with one stage, the main sensor and one reference sensor

This section is about measuring the optical flat with one stage, the confocal sensor (main sensor) and one capacitive sensor (reference sensor). The sensor naming and placement are defined in figure 14 in section 3.2.3. The confocal sensor is denoted by m_1 , and capacitive sensors are denoted by r_1, r_2 and r_3 . Only one capacitive sensor is used as reference sensor to compensate for inaccuracies. Since only one sensor is used, no distinction between z , R_x and R_y can be made in the reference measurement. Due to this, only z error compensation can be done. This test is done to check the effect by adding one reference sensor. The results are then compared to the results of subsection 3.5.1.

Expected If the stage would only have an inaccuracy in z but not in R_x or R_y , one reference sensor would sufficient as stage inaccuracy compensation. The manufacturer specifies a maximum pitch / roll inaccuracy of 140 μrad , so it is expected that the stage will have R_x and R_y inaccuracies. A calculation on the effect of pitch/roll inaccuracies is done in section 2.2. The sensors are 0.02m apart, thus the maximum expected inaccuracy in z due to R_x is the following: $z = \alpha * L = 140\mu\text{rad} * 0.02 = 2.8\mu\text{m}$. Since the inaccuracy in R_x and R_y cannot be measured with one reference sensor while the error in z can be measured, the expected inaccuracy after subtracting the reference sensor from the main sensor is 2.8 μm maximum. The manufacturer of the stage does not specify whether the inaccuracy has the same magnitude in both R_x and R_y . Due to the fact that it is unknown whether the stage is dominated by R_x and R_y , it is expected that the reference sensor placement with respect to the main sensor placement does influence the results.

Implementation The optical flat will be measured similarly as described in subsection 3.5.1, but with a measurement pitch of 2000 μm . Instead of using one sensor, two sensors are being used. As addition to the confocal sensor (main sensor), the capacitive sensor (reference sensor) will be used to compensate for stage inaccuracies in z . The absolute distance of each measurement point of the capacitive sensor will be subtracted from the confocal sensor. The capacitive sensors can be either on location r_1, r_2 or r_3 . As explained above, it is expected that the placement of the reference sensor with respect to the main sensor influences the result. The reference sensor will therefore be placed on location r_1, r_2 and r_3 in three separate measurements. The

measurement data of each reference sensor will be subtracted from the main sensor separately, which leads to three different results.

Results Figure 26 shows the results of after subtracting the data from either capacitive sensor (r_1 , r_2 or r_3) from the data of the confocal sensor (m_1). Since both the confocal sensor as the capacitive sensor measure the optical flat, a perfect error compensation would result in a signal with a horizontal line (with a few hundred nanometers deviation due to imperfections in the optical flat and sensor measurement errors). Since Rx and Ry are not compensated for, the expected maximum deviation after subtracting the measurement data is $2.8 \mu\text{m}$ plus a few hundred nanometers due to the above mentioned errors. Figure 26 shows that compensating from either locations (r_1 , r_2 or r_3) results in a measurement inaccuracy with the order of the expected deviation due to Rx and Ry. It can be seen that using the capacitive sensor on location r_2 results in the best stage inaccuracy compensation, since the line deviates the least ($0.6 \mu\text{m}$). The worst case would be on the location of r_1 , which gives a deviation of $1.5 \mu\text{m}$. When comparing the measurement data with the measurement data from section 3.5.1, it can be seen that the data is improved from $3 \mu\text{m}$ error to $1.5 \mu\text{m}$.

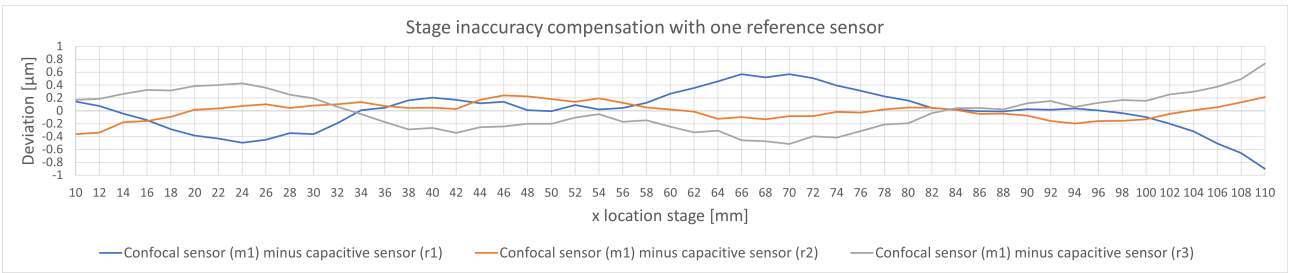


Figure 26: Confocal sensor (main sensor) minus capacitive sensor (reference sensor)

3.5.4 Measuring with one stage, the main sensor and three reference sensor sensors

In this section the optical flat is measured with the confocal sensor (main sensor) and three capacitive sensors (reference sensors). Since three reference sensors are used, z, Rx and Ry stage inaccuracies can be measured. The main sensor is used to verify the result by measuring with a fourth sensor.

Expected Since all three stage inaccuracies can be measured by the three reference sensors, it is expected that the stage inaccuracies can be compensated for. The confocal sensor will be used to verify the results. The remaining errors still left in the system are the following:

- The flatness of the optical flat, which is $<60 \text{ nm}$.
- The error in the sensors, which is expected to be $\ll 600 \text{ nm}$, since the error of 500 nm would be over the whole range of the sensor (see subsection 3.3.1).
- Since the measurement only takes about 2 minutes, it is not expected that temperature deviation will cause an additional error.
- The measurement is a relative measurement between the reference sensors and the main sensors. The previously described screw spindle error will therefore have no influence on the measurement.

After adding the errors, the maximum error measured is expected to be $\ll 660 \text{ nm}$.

Implementation The optical flat will be measured on a similar manner as done in the previous two tests (subsection 3.5.1 and subsection 3.5.3), but with three reference sensors. Figure 27 the introduces uvw-coordinate system. The uvw-coordinate system is introduced to indicate the location of the sensors with respect to each other. The origin of the coordinate system is on the location of the confocal sensor, while the three reference sensors are on a circular pattern of 120 degrees. To be able to subtract the data of the three reference sensors from the main sensor, some algebra is required. The three reference sensors span a plane in the 3D uvw space. The u and v coordinates of the sensors are known, since the sensors are located on a defined location in the sensor holder. The w component is the sensor is the absolute measured distance from sensor to the optical flat. As all three components of the reference sensors are known, a plane can be fit through the three sensors.

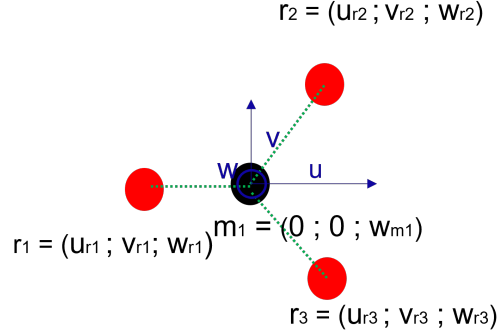


Figure 27: Sensor placement and naming with uvw coordinate system

The equation of a plane is $a * u + b * v + c * w = d$. Once the a,b,c and D are known, the w value of the plane on each uv location can be determined easily. To get the a, b and c components of the equation of the plane, some linear algebra is used. The components a, b and c are the components of the normal vector of the plane. The normal vector \mathbf{n} of the plane is thus defined as the following: $\mathbf{n} = (a \ b \ c)^T$. To obtain the normal vector, the cross product of two arbitrary vectors on the plane can be taken. The first vector is \mathbf{R}_1 from r_1 to r_3 , the second vector is \mathbf{R}_2 from r_1 to r_2 . Vector \mathbf{R}_1 can be obtained by subtracting r_3 from r_1 component wise and vector \mathbf{R}_2 can be obtained by subtracting r_2 from r_1 component wise. Since two vectors on the plane are known, the normal vector is calculated; $\mathbf{n} = \mathbf{R}_1 \times \mathbf{R}_2 = (a \ b \ c)^T$. By filling in a point on the plane (r_1, r_2 or r_3) together with a, b, c, the last unknown, d, is found. After rewriting the equation of the plane for w ($w = \frac{d - a * u - b * v}{c}$), on any location of the uv plane a value for w can be determined. This is the value for the reference plane, thus stage inaccuracy on that specific point on the uv plane. As can be seen on figure 27, the location of the confocal sensor (main sensor m_1) is in the origin of the uv plane. To correct for stage inaccuracies, the value of the reference plane at the location of the confocal sensor is subtracted from the absolute measurement value of the confocal sensor. Since the optical flat is measured by all four sensors, theoretically the result should be a horizontal line with an error of «660nm as described above.

Results The results of the measurement can be seen in figure 28. The figure shows all individual sensor measurement data and the calculated resulting flatness as described above. The average of each individual sensor is subtracted from that specific sensor, to transform the absolute measurement to relative measurement.

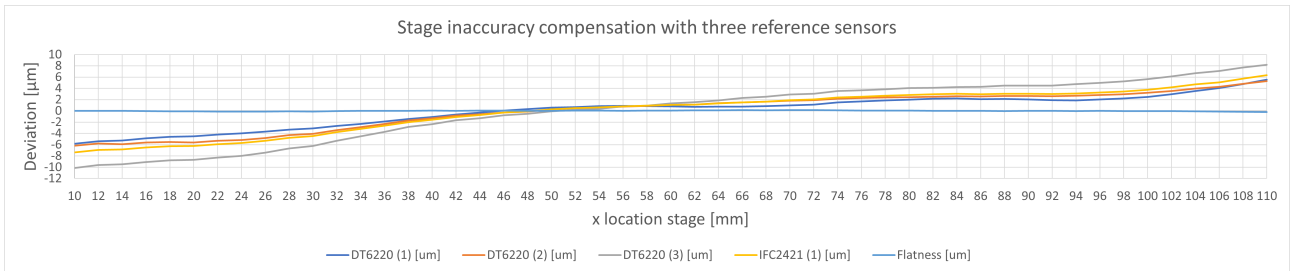


Figure 28: Measurement with all sensors and calculated flatness

The blue line which indicates the flatness shows an improvement in comparison with the measurement data of the main sensor. Figure 29 shows the same flatness result, but with a different y-axis scaling. The remaining deviation is $0.10 \mu\text{m}$, which is within the expected results of $\ll 0.66 \mu\text{m}$. During first measurements the results were worse, for which a sensor validation test is done as described in section 3.6.3. After performing the validation, the confocal sensor showed significant errors, which were resolved by properly connecting the sensor cable.

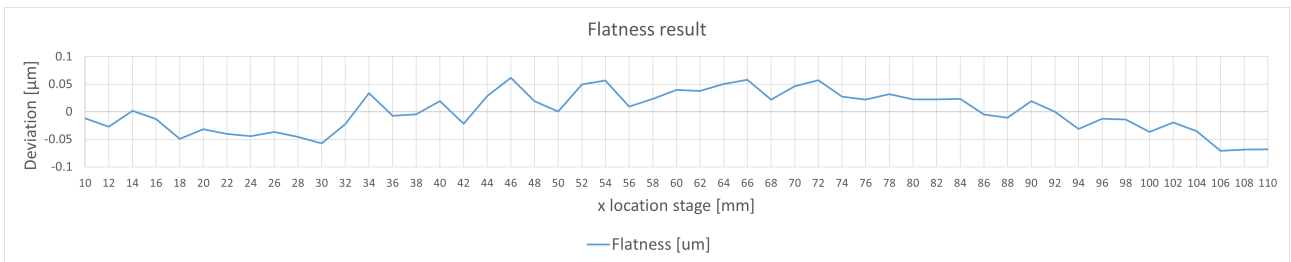


Figure 29: Flatness measurement all sensors

Finally, pitch and roll of the stage are determined. based on the three reference sensor. As can be seen, the pitch (R_x) is roughly $130 \mu\text{rad}$ and the roll (R_y) is roughly $100 \mu\text{rad}$ over the measured range. When using three reference sensors, this in theory is all accounted for, while R_x and R_y cannot be accounted for when using 1 reference sensor.

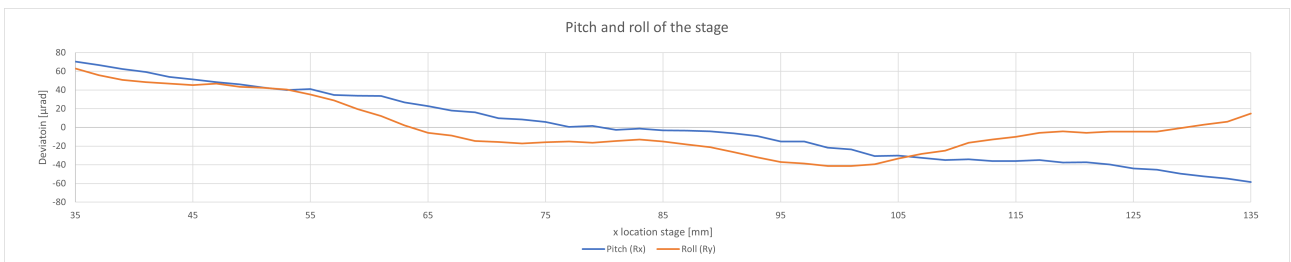


Figure 30: Pitch and roll measured by the capacitive sensors

3.5.5 Measuring with two stages and the main sensor

This test is done to verify the system using two stages and one sensor (system 1 as described in section 2.1). To reduce sensor errors, the used sensor measurement range must be as small as possible. In order to reduce the measurement range of the sensors, the optical flat must be parallel with the movement of the stage.

Expected The optical flat is not expected to be parallel to the xy-plane of the movement of the stage. As the optical flat is not parallel, more measurement range will be used by the sensors, thus the bigger the error of the sensors will be. It is expected that the error of the confocal sensor is reduced if the top side optical flat is parallel with the movement of the stage. The measurement is expected to be dominated by the stage inaccuracies if the optical flat is placed parallel to the movement of the stage.

Implementation First, the optical flat will be placed on the stages and measurements will be done in a grid pattern. The grid will be a grid of 60x60 mm with a pitch of 2mm between measurement points. The measurements will show whether the optical flat is tilted physically. The tilt will be reduced by shimming the optical flat in order to reduce sensor errors. In order to analyze the data, the remaining tilt of the measurement data will be removed by subtracting a linear fit through the measured data, from the measurement data. The result will be a relative flatness measurement of which the tilt is removed.

Results Figure 31 shows the measurement result of the optical flat which is measured by just the confocal sensor. As can be seen, the optical flat has a tilt with a delta z of approximately $55 \mu\text{m}$ over the measured range. This tilt is probably introduced due to stacking of the two stages. The tilt of the optical flat is reduced by putting a shim under the lower side of the optical flat. After physically reducing the tilt, the measurement of the confocal sensor is as shown in figure 32 (notice the range of the height has changes). A tilt is still observed, but the tilt is reduced from roughly 55 micron to 15 micron.

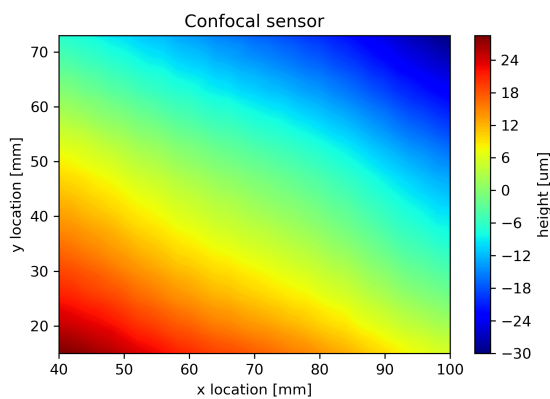


Figure 31: Confocal sensor with tilt

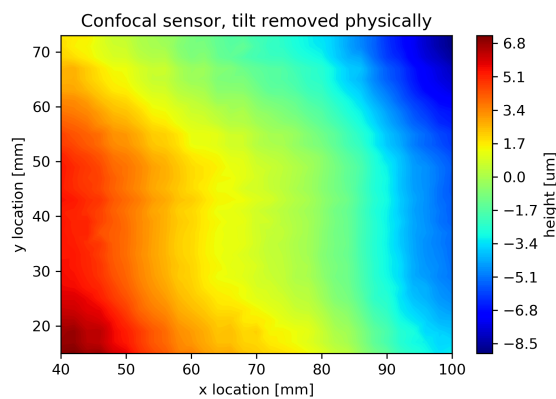


Figure 32: Confocal sensor tilt removed

Finally, the remaining tilt is removed by subtracting a linear plane fit from the data. The result of the measurement is shown in figure 33. The result is a deviation of roughly $3.2 \mu\text{m}$, which is expected to be mainly dominated by stage inaccuracies.

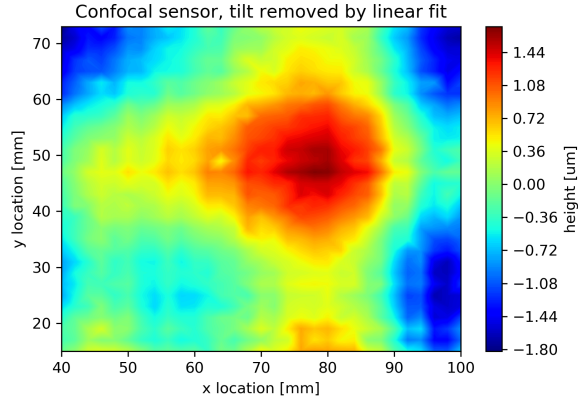


Figure 33: Confocal sensor tilt removed by linear fit

Similar to section 3.5.1, a distinction between random and reproducible stage inaccuracies can be made by subtracting two measurements.

3.5.6 Distinction of random and reproducible stage inaccuracies with two stages

The method described in this research does not only compensate for reproducible inaccuracies, but also random inaccuracies. Random inaccuracies are obviously difficult to account for, since these have to be measured simultaneously when determining flatness based on point-wise measurements. If no reference sensor would be used and the stage error could be mapped by measuring an optical flat prior to a sample, the remaining error will be the random error. So when doing this calibration method, the reproducible inaccuracies are accounted for. This test is done to make the distinction between random and reproducible stage inaccuracies by subtracting different measurements of capacitive sensors from each other. The result of this subtraction will lead to the random stage inaccuracies. The confocal sensor is used to make the distinction between the random and reproducible inaccuracies.

Expected In section 3.5.1, the random stage inaccuracies for one stage were found to be $0.3 \mu\text{m}$. Since the contribution of random stage inaccuracies was $0.3 \mu\text{m}$ for one stage, it is expected to be around $0.6 \mu\text{m}$ when the two stages are combined.

Implementation Similar to previous section the optical flat will be measured by measuring a grid of 60×60 mm with a pitch of 2 mm with the confocal sensor. Two measurements will be done per day on two different days, which leads to four measurements in total. The measurement of two different measurements will be subtracted from each other. The result will be the contribution of random stage inaccuracies.

Result Down below in table 3 an overview of the 4 measurements is shown. Measurement 1 and 2 are on the same day, and measurement 3 and 4 are on a different day. The table shows the row minus column, so for example location (1,3) as (row,column) is measurement 1 minus measurement 3. The value which is left is the difference between the global maximum and global minimum of the plane measurements. Two examples of these plots are shown in figure 34 and figure 35. Although the grid of measurements of 2x2 mm can be seen clearly, the corresponding height values are random as expected. The average random stage inaccuracy leads to 1.0 μm , which is higher than expected. When using just one sensor to account for reproducible inaccuracies (calibration method) the remaining inaccuracy will be 1.0 μm , since these are random inaccuracies.

	Measurement 1	Measurement 2	Measurement 3	Measurement 4
Measurement 1	-	0.9 μm	1.0 μm	1.0 μm
Measurement 2	0.9 μm	-	0.9 μm	1.0 μm
Measurement 3	1.0 μm	0.9 μm	-	1.0 μm
Measurement 4	1.0 μm	1.0 μm	1.0 μm	-

Table 3: Random stage inaccuracy measurement

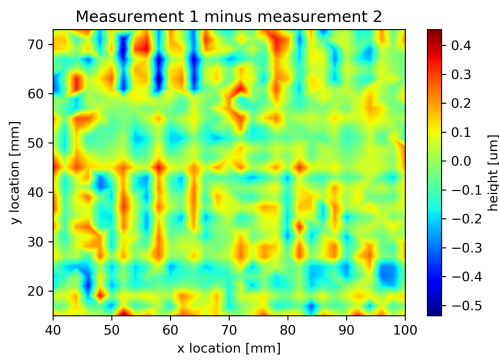


Figure 34: Random error measurement 1 minus measurement 2

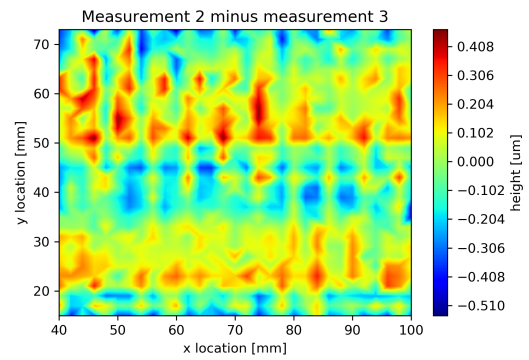


Figure 35: Random error measurement 2 minus measurement 3

3.5.7 Measuring with two stages, the main sensor and one reference sensor

This section describes the measurement of the optical flat with two stages, the main sensor and one reference sensor to measure stage inaccuracies (which corresponds with system 2 from section 2.2). The measurement data from the capacitive sensor will be subtracted from the confocal sensor in order to check the improvement of adding one reference sensor to the configuration without a reference sensor.

Expected Since the tilt of the optical flat is reduced, the error of the sensors is minimized, but still present. It is expected that the location of the capacitive sensor will impact the results on the measurements. In the section 3.5.5, the stage inaccuracies for the combined stages measured with the confocal sensor were roughly $3.2 \mu\text{m}$. Since one sensor is used as reference sensor, the error is expected to be reduced. The remaining inaccuracy is expected to be between 1 and $3.2 \mu\text{m}$.

Implementation The measurement will be done in a grid pattern. The grid will be a grid of $60 \times 60 \text{ mm}$ with a pitch of 2 mm between the measurement points. The capacitive (reference) sensor will be located on sensor locations r_1 , r_2 and r_3 (as previously shown on figure 27). The sensor data of each capacitive sensor location will be subtracted from the measurement of the confocal (main) sensor.

Results Figure 36 shows the result after subtracting the capacitive sensor on location r_1 from the confocal sensor. The minimum measured stage inaccuracy is about $1.2 \mu\text{m}$. For the measurements with the capacitive sensor on location r_2 (figure 37) the remaining inaccuracy is $1.3 \mu\text{m}$ and for location r_3 (figure 38) it is $1.6 \mu\text{m}$. All three measurements are an improvement when compared with the results without any stage inaccuracy compensation. The result without any stage inaccuracy compensation was a deviation of $3.2 \mu\text{m}$. The results of using a reference sensor are not an improvement in comparison with using the calibration method to account for random stage inaccuracies, which resulted in a remaining inaccuracy of $1 \mu\text{m}$ (as described in section 3.5.6).

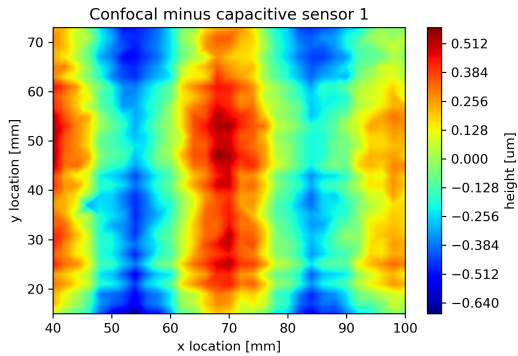


Figure 36: Confocal minus capacitive sensor on location r_1

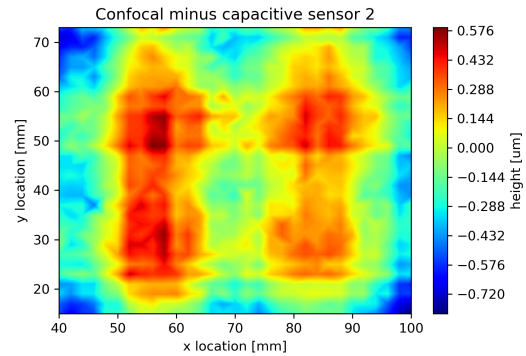


Figure 37: Confocal minus capacitive sensor on location r_2

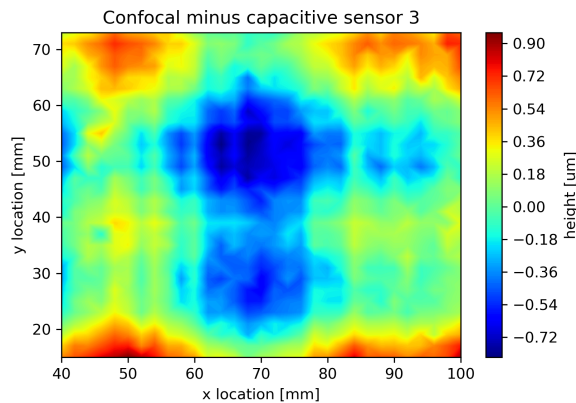


Figure 38: Confocal minus capacitive sensor on location r_3

3.5.8 Measuring with two stages, the main sensor and three reference sensors

This section describes the system with two stages, the main sensor and three reference sensors. This system corresponds with measurement system 3 (subsection 2.3), and is the final setup. Since three reference sensors are used, z, Rx and Ry stage inaccuracies can be measured and accounted for. The main sensor is used to verify the results by measuring with a fourth sensor.

Expected Since all stage inaccuracies can be measured and accounted for, it is expected that the remaining measurement signal only consists of the following errors:

- The flatness of the optical flat, which is $< 60\text{nm}$.
- While the physical tilt of the optical flat is minimized, sensor errors are still expected to be present. The total sensor error is expected to be $\ll 600\text{ nm}$.
- Since the measurement only takes 20 minutes, it is not expected that temperature deviation will cause an additional error.
- The measurement is a relative measurement between the reference sensors and the main sensors. The previously described screw spindle error will therefore have no influence on the measurement.

The total error is therefore expected to be $\ll 660\text{ nm}$ (or $\ll 0.660\text{ }\mu\text{m}$). The pitch (Rx) and roll (Ry) will also be measured by the three capacitive sensors. The expected value is $< 280\text{ }\mu\text{rad}$, since this is the maximum specified pitch/roll by the manufacturer when using two stages in xy-configuration.

Implementation The measurement will be done in a grid pattern. The grid will be a grid of 60x60 mm with a pitch of 2 mm between the measurement points. The three reference sensors will be placed on locations r_1 , r_2 and r_3 and the main sensor will be placed on location m_1 , as described in figure 27. The data from the three reference sensors will be deducted from the main sensor in order to validate the system. To determine the pitch (Rx) and roll (Ry), the three reference sensors will be used.

Results The results will be analyzed similar to the configuration with 1 stage and three reference sensors (see subsection 3.5.4). The measurement signal of the three reference sensors will be combined and subtracted from the signal of the confocal sensor. Figure 39d shows the result of this analysis. Temperature was constant during during the test, which took about 20 minutes. A high and low peak are observed in the measurements, which are likely a dust particle and a small scratch on the optical flat. The two white areas on the figure were the location of this dust particle and the scratch. After removing the two imperfections from the data, the remaining inaccuracy is $0.13 \mu\text{m}$. The results of previous tests are repeated down on figure 39a (no reference sensor), figure 39b (calibration method) and figure 39c (1 reference sensor). Note that the scaling of the figures changes by looking at the color bar. It can be seen that the remaining measured inaccuracy of the method with 3 reference sensors is improved with respect to the other methods. As addition to the inaccuracy in z, the inaccuracies Rx and Ry are measured and determined by the three reference sensors. Both the pitch (Rx) and roll (Ry) are measured by the capacitive sensors and are $85 \mu\text{rad}$ and $150 \mu\text{rad}$ respectively. Both Rx and Ry inaccuracies are lower then expected.

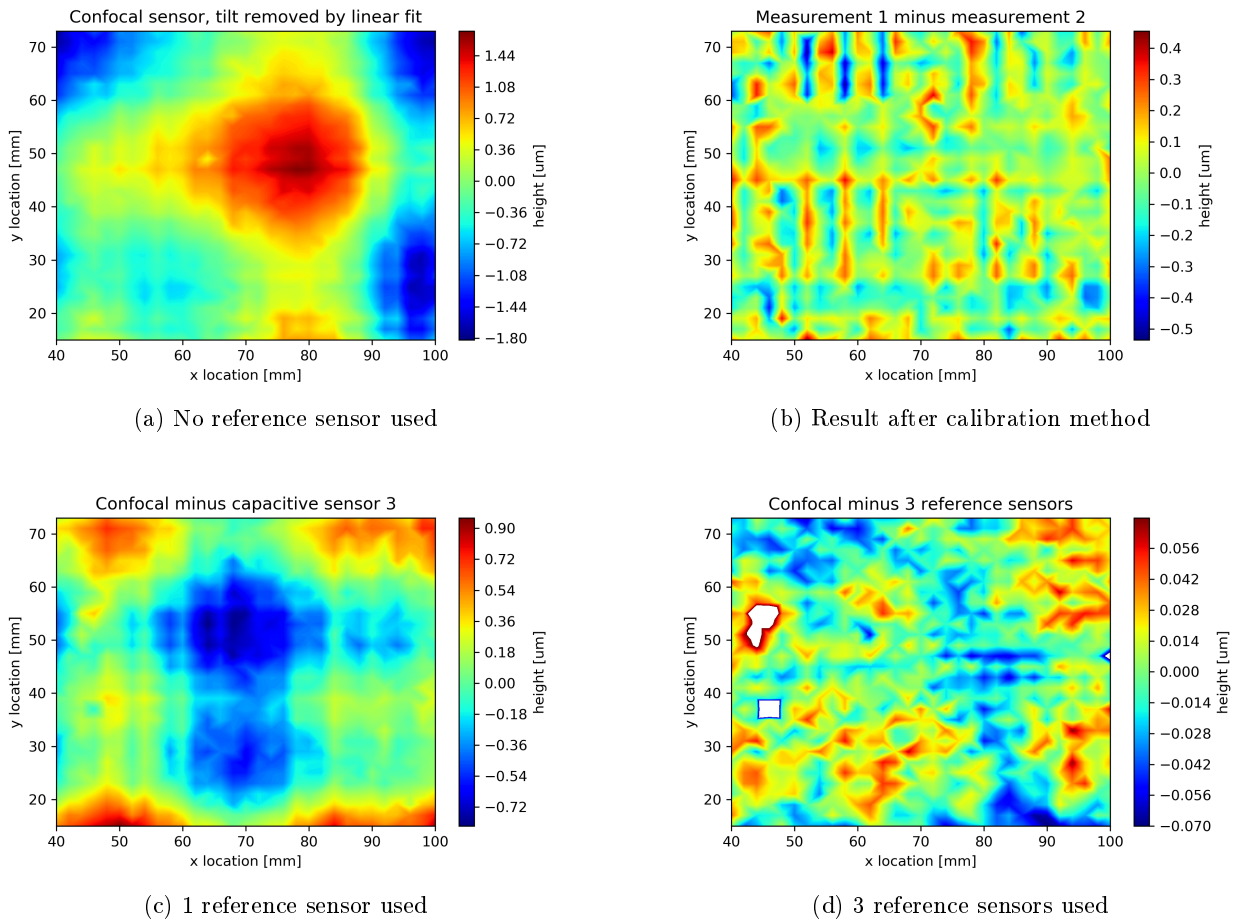


Figure 39: Overview of the results (note the change in the scale of the height bar)

3.6 Experimental optimization

This section describes the experimental optimization which is done throughout the research.

3.6.1 3D printed parts

For the production of both the sensor holder as optical flat holder, additive manufacturing is used for prototyping. The parts were 3D plastic printed by an FDM printer. During the tests it was noticed that the setup did not behave as expected. The dimensions of the printed parts are expected to function with the feasibility demonstrator, since the parts are designed to function while printed with a 3D plastic printer which has worse tolerances in comparison with other manufacturing methods. The parts are made out of PLA, which is a commonly used plastic in additive manufacturing. PLA has a thermal expansion coefficient of $68 \frac{\mu m}{m \cdot K}$, which roughly 3 times higher than aluminum ($22 \frac{\mu m}{m \cdot K}$). Apart from the higher thermal expansion coefficient, 3D printed parts are often printed partly hollow. Due to both of these facts, 3D printed parts are expected to react strongly and unpredictable on temperature fluctuations. Down below in figure 40, the behavior of the sensors can be seen during a 48 hours period. The temperature deviation can be seen in figure 41. As can be seen, during temperature fluctuations, especially capacitive sensor 2 and capacitive sensor 3 show relatively big deviations. Sensor 2 and 3 have the greatest distance with respect to the attachment point of the setup, which is why deviations are relatively big. Since it is of importance for the sensors to behave similar with respect to each other, the 3D printed parts are not behaving as required. For this reason, the 3D printed parts are replaced with CNC milled parts made out of aluminum, which gave better results as can be seen in section 3.4.1.

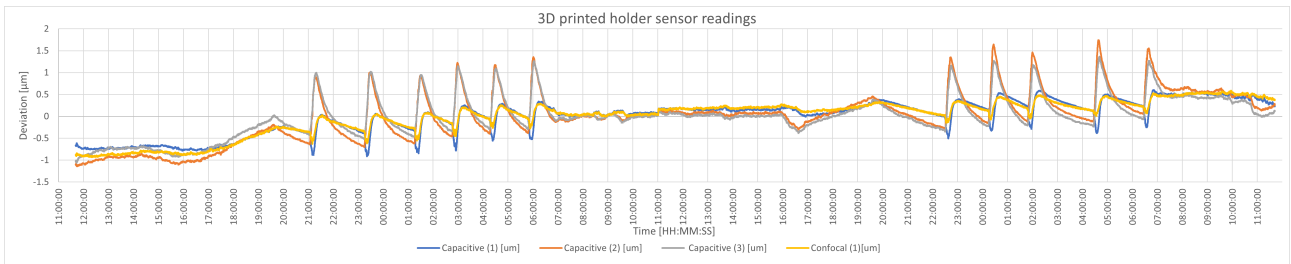


Figure 40: 3D printed parts sensor behavior test

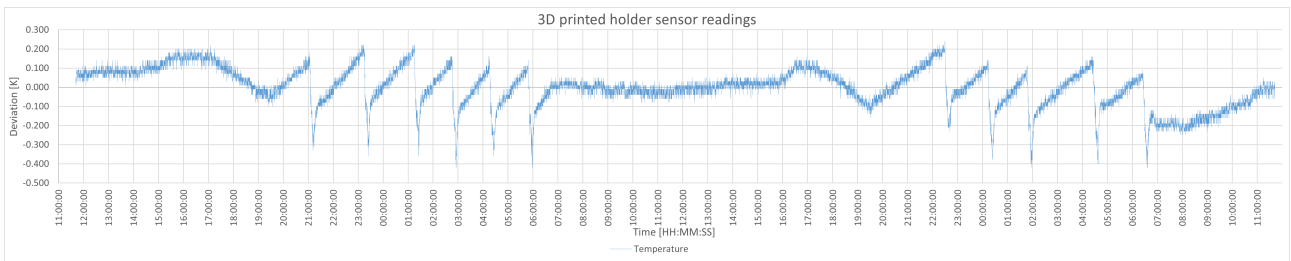


Figure 41: Temperature during test

3.6.2 Test the sensor on receiving a value

The sensors which are used for measuring the optical flat, denoted as reference sensors, are capacitive sensors with a measurement range of $500\ \mu\text{m}$. The range starts at $1\ \mu\text{m}$ and ends at $500\ \mu\text{m}$ from the sample. The sensor which is used to measure the sample, denoted as sample sensor, is a confocal sensor with a measurement range of $800\ \mu\text{m}$. The working distance is from 5.94mm to 6.74mm . The sensors require to be within the measurement range, so placement of the sensor with respect to the measurement object is relevant. It is expected to be able to position the sensor within measurement range. The positioning of the sensor will be done by using a feeler gauge. A feeler gauge is a tool which is usually used to measure clearances between gaps. A feeler gauge consists of several steel parts with varying thicknesses stacked together on a hinge. In this case, the different thicknesses of the feeler gauge are used to place the sensor at a certain distance from the optical flat. The feeler gauge comes in steps of $10\ \mu\text{m}$ from $30\text{-}100\ \mu\text{m}$ and steps of $50\ \mu\text{m}$ from $100\text{-}1000\ \mu\text{m}$, it is expected to put the sensors atleast within $50\ \mu\text{m}$ in range with respect to each other. The readings on the sensor will confirm whether this is the case. The sensors are not required to be set on equal distance of the optical flat with respect to each other, since the measurements are absolute measurements. As explained above, a feeler gauge is used to align the sensor within measurement range of the optical flat. Figure 42 shows a schematic of using the feeler gauge to align the capacitive sensors. Since the optical flat is gold coated, the surface is scratched easily. To prevent damaging the optical flat as well as the sensors, the feeler gauge is taped with kapton tape on both sides. The measurement range of the capacitive sensors are $500\ \mu\text{m}$. According to the manufacturers calibration rapport, the ideal distance from the sample is $200\ \mu\text{m}$. The $100\ \mu\text{m}$ feeler gauge is used with the kapton tape on both sides. The total thickness of the feeler gauge is roughly $220\ \mu\text{m}$. It is expected that a value of roughly $220\ \mu\text{m}$ is read on the sensor readings. For the confocal sensor, there isn't an ideal distance according to the calibration rapport. As the confocal sensor requires a range of 6.34mm to be in the middle of the measurement range, a 6mm 3D printed part is used (see figure 43). This would require a feeler gauge of $200\ \mu\text{m}$, which would be $320\ \mu\text{m}$ with kapton tape.

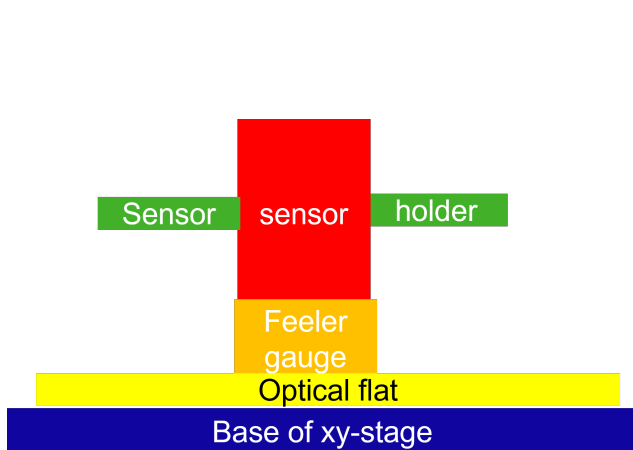


Figure 42: Sensor alignment with optical flat capacitive sensor

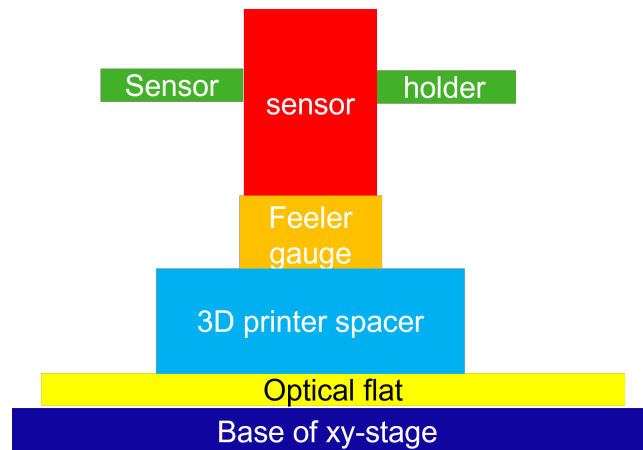


Figure 43: Sensor alignment with optical flat confocal sensor

Although the method works well in terms of getting the sensors in the measurement range, it does result in small scratches on the optical flat. Since the confocal sensor has a spotsize of $6\ \mu\text{m}$, scratches are measured by it. Due to this, scratches are not desirable. The kapton tape which is on the feeler gauge still has some sharp edges after cutting it, which cause scratches. Fortunately an old optical flat is used to test the method, so scratches did not matter much. The second method used is sliding the sensor by hand and tighten the set screw when the software readings are at the desired value. The sensor placement by this method prevents anything from touching the optical flat, which leaves the optical flat in tact. The sensors are place within a range of $10\ \mu\text{m}$ with respect to each other.

3.6.3 Sensors validation

The initial results of section 3.5.4 showed that one or more sensors are showing wrong measurement results due to measurement errors. After doing some tests, the hypothesis got more specific. The hypothesis is the following: *Measurement errors are present because the confocal sensor sensor is measuring in more of the measurement range and therefore has a bigger linearity error.* This test is done to validate the errors when using the sensor in more measurement range. As tested in subsection 3.3.1, the sensors gave repeatable measurements when measuring the optical flat. During the repeatability test, the absolute distance between the sensors and the optical flat did not change. Since the absolute distance did not change, the sensor is validated when using more measurement range. Sensor errors, such as linearity errors, increases once more of the measurement range is used. Due to this, it is expected that the error of the sensor increases once the used measurement range is increased.

First the optical flat is regularly measured with all 4 sensors, similar to section 3.5.4. To use more of the measurement range of the sensors, a tilt of the optical flat is introduced. To introduce this tilt, a shim will be placed under the optical flat as shown in figure 44. The shim has a thickness of $50\ \mu\text{m}$, thus should introduce a tilt with a height difference of approximately $50\ \mu\text{m}$ over the range of the optical flat (resulting in approximately $300\ \mu\text{rad}$). The measured signal after introducing the tilt will contain stage inaccuracies, flatness error of the optical flat, sensor errors and the tilt. As shown in section 3.5.1, most of the stage inaccuracies are reproducible. Since most inaccuracies are reproducible, the reproducible stage inaccuracies will be removed once the signal from the regular measurement is subtracted from the tilted measurement. The signal which is left would be a straight line, since the optical flat is tilted. The deviations from this linear line indicate the errors due to the flatness of the optical flat, the random errors of the stage and sensor errors. Since the optical flat has a flatness of $<60\ \text{nm}$ and the random errors are $<300\ \text{nm}$, all deviations from the linear line with readings $>360\ \text{nm}$ are due to sensor errors. Since the results in section 3.5.4 were off by approximately $1\ \mu\text{m}$ while still being in a relative small measurement range of the confocal sensor (12 out of $800\ \mu\text{m}$), it is expected that the sensor errors in this test (with a measurement range of approximately 65 out of $800\ \mu\text{m}$) will be $>1\ \mu\text{m}$.

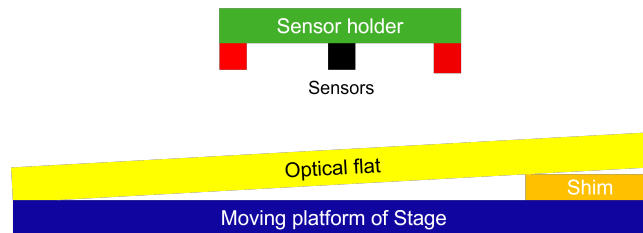


Figure 44: Optical flat tilt by shim

Down below the results are shown. First a regular measurement with all four sensors is done without the addition of a shim, which is shown in figure 45. After adding a shim on the right side (as shown in figure 44) and doing the measurement, the result is plotted as can be seen on figure 46. The optical flat is tilted with approximately $60 \mu\text{m}$ as expected, notice that the y-axis has changed. On figure 46 the result of subtracting the data without a shim (figure 45) from the data with a shim (figure 46) can be seen. After "rotating" the graph by subtracting a linear fit from the data, the sensor error can be seen on figure 48. It can be seen clearly that the confocal sensor has errors ($\pm 4 \mu\text{m}$) which are out of spec ($< \pm 0.2 \mu\text{m}$). The capacitive sensors all have a deviation of $\pm 0.2 \mu\text{m}$, which is almost in spec ($< \pm 0.15 \mu\text{m}$). This confirms the hypothesis that the sensor is giving the wrong results. Due to the tilt, two factors are changed. The sensor uses more of the measurement range and the sensor has a bigger measurement angle. The angle change due to the shim is roughly $\ll 1^\circ$, while the sensor should handle a tilt angle of $\pm 35^\circ$. The measurement error is therefore expected to have the error rather due to using more measurement range then increasing the angle of due to tilting the optical flat. After inspecting the confocal sensor, the cause of the error is found. The cable of the sensor was not connected properly. After connecting the cable properly, the observed error in the confocal sensor is resolved.

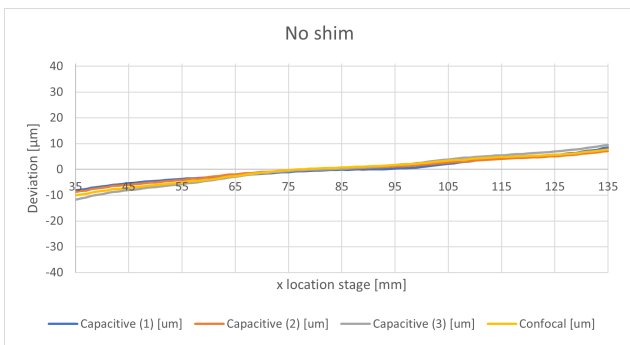


Figure 45: No shim

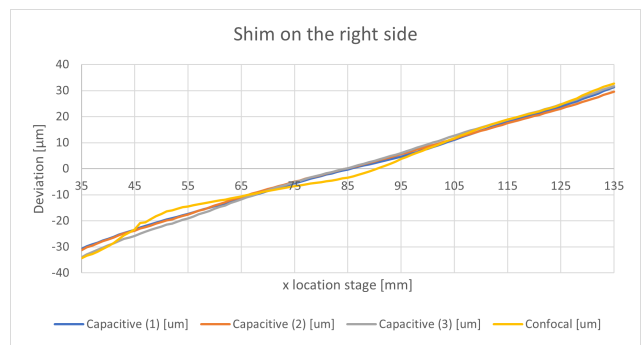


Figure 46: 1 shim on the right side

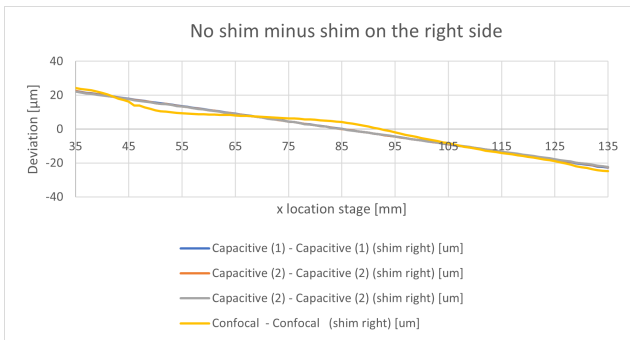


Figure 47: No shim minus one shim right

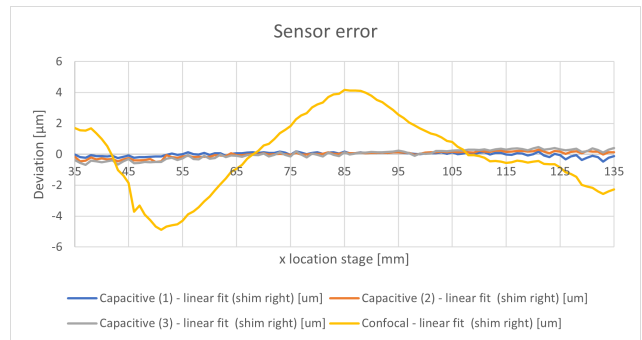


Figure 48: Sensor error

Chapter 4: Discussion and recommendations

This chapter contains the discussion with recommendations for improvement of performance, conclusions and recommendations for further research. During the discussion, the results from the tests of the previous chapter will be discussed and improvements on performance will be stated. Secondly, the research conclusions can be found in section 5.1. Finally recommendations for further research can be found in section 5.2.

4.1 Discussion and recommendations for improvement of performance

This section discusses the results found in the previous chapter. First the thermal effects and measurement pitch determination are discussed, after which the sensor errors are evaluated. Secondly the results on the xy-stage inaccuracies with and without reference sensors are reviewed. Finally the limitations of the setup will be considered and recommendations for improvement of performance will be given.

4.1.1 Thermal effects

Thermal effects were expected to have significant influence on the measurement data. The changing ambient temperature and distance sensor data have been monitored for 48 hours to verify the thermal effects. During this test a clear correlation between temperature and measured distance is noticed. Within the observed temperature deviation of 0.35 K, the sensor values deviated at most 300 nm. Since the principle of the setup is comparing the relative distance measurement of the confocal sensor with the three capacitive sensors, it is of importance that the sensors behave in the same relative matter when temperature changes. During this period of 48 hours, the sensors deviate with a value of 50 nm with respect to each other. Due to this, the added error due to temperature deviation is 50 nm. This is acceptable within the boundary of this research. Stage warm-up effects due to movement of the stage were also expected to influence the measurement data. For the specific linear stages used during this research, warm-up effects due to movement of the stage did not have significant influence on the measurements. This could be different for other types of linear stages and settings, so it is recommended to look into when using a different setup. As the thermal effects are known, the setup has been tested further.

4.1.2 Determine measurement pitch

Although the goal of the setup is to measure the flatness of a surface, first only one stage has been used to measure the flatness of a line. This has been done to determine the measurement pitch and to build up in complexity of the setup and analysis. The measurement pitch has been determined to find an optimum between measurement time and minimum required data acquisition. The amount of measurement points increases quadratically with a decrease in pitch distance. The measurement time scales linearly with the amount of measurements points, so measurement pitch is of influence on the measurement time with a quadratic behavior. Increasing the measurement pitch distance results in less measurement points, thus less data. The pitch could be determined based on measurement time or on expected spatial frequencies of the stage inaccuracies. The stage has been characterized by measuring an optical flat with a fine measurement pitch, which shows inaccuracies with both low and high spatial frequencies. A course pitch causes loss in measurement of stage inaccuracies with a high spatial frequency, since these are not measured. During the research an inaccuracy with a high spatial frequency is measured, which is the screw spindle of the stage with a which has a period of 1 mm. Since the stage inaccuracy caused by the screw spindle had a low amplitude, a more course measurement pitch is chosen. Similar errors could be found on any setup with a stage by first characterizing the inaccuracies by measuring it with a fine pitch. An appropriate pitch can then be determined based on the frequency of the inaccuracy and the introduced errors due to not measuring the error with a more course pitch. In order to correctly measure the amplitude of an inaccuracy, the pitch must be an order lower than the period of the inaccuracy which is to be measured.

Apart from the measurement pitch, the spot-size of the sensor also influences the ability of measuring certain high frequent errors. Whether the spot-size of the sensor has influence on the measurement data, depends on the cause of the measured inaccuracy. If high frequent inaccuracies are present on the surface under test, the spot-size also determines whether the inaccuracies can be measured. High frequent stage inaccuracies can however still be measured with a big spot-size, since the whole surface under test moves with the stage inaccuracy. Figure 49 shows the difference between high frequent inaccuracies on the stage trajectory (left) or high frequent inaccuracies on the surface (right). During this research, the capacitive sensor are sensors used with a relatively big measurement spot-size. Due to this big spot-size, high frequent inaccuracies on the surface under test during cannot be measured. Fortunately the surface under test is an optical flat, which is expected

to have a low frequent inaccuracy. If a surface is measured in a practical environment, this should be taken into consideration.

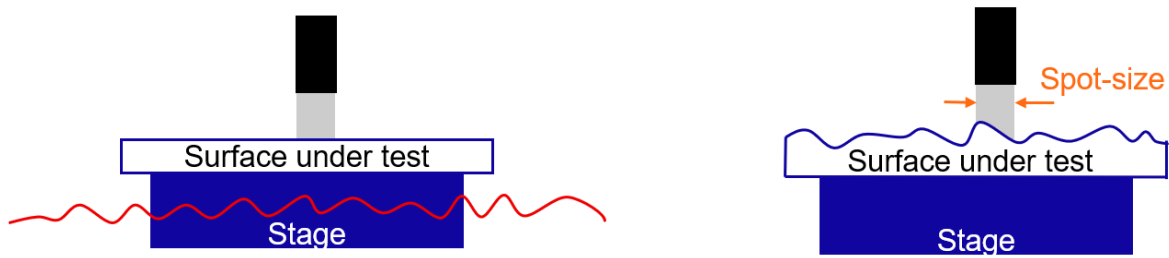


Figure 49: Effect of spot-size on high frequent inaccuracies

4.1.3 Sensor errors

As the setup has been measured with one stage, the main sensor and three reference sensors, remaining measurement errors have been observed. To keep this error to a minimum, the usage of measurement range of the sensors had to be reduced. Since an increase in tilt of the optical flat leads to an increase in measurement range of the sensor, this tilt had to be reduced by shimming the optical flat which reduced the used sensor range to $15 \mu\text{m}$. The lesson learned here is to always test the specifications provided by the manufacturer when possible. If a new or different sensor would be available, the sensor could be tested on repeatability and on errors. The test on errors will be done by using a stage to systematically go from the start to the end of the measurement range of the sensor by using a linear stage (as shown in figure 50). A downside of this method is that the stage accuracy along the axis of movement (y in this case) is of importance.

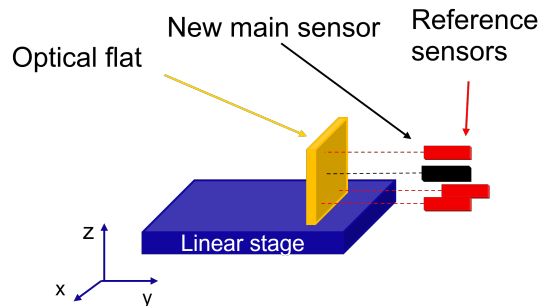


Figure 50: Sensor test on errors

4.1.4 Random and reproducible xy-stage inaccuracies

By measuring the optical flat on the xy -stage, the measured inaccuracy in z is $3.3 \mu\text{m}$. The pitch (R_x) and roll (R_y) of the stage has also been measured, which are $85 \mu\text{rad}$ and $150 \mu\text{rad}$ respectively. This measurement contains both stage inaccuracies and a summation of introduced errors. These errors are errors by the sensors, the optical flat not being perfectly flat and not measuring the screw spindle error due to a relatively high spatial measurement distance. The measured stage inaccuracies can be split into random and reproducible stage inaccuracies. The measurement method described in this research does not only compensate for reproducible inaccuracies, but also compensates for random inaccuracies. Random inaccuracies are obviously more difficult to account for, since these have to be measured simultaneously when determining flatness based on point-wise measurements. The total inaccuracy is divided in random and reproducible inaccuracies by measuring the optical multiple times with a capacitive sensor and subtracting these measurements. The random inaccuracies have been determined to be $1.0 \mu\text{m}$ and is expected to be dominated by stage inaccuracies rather than sensor errors, since the performance of the system increased by using three reference sensors. If no reference sensor is used and the stage inaccuracy would be mapped by measuring an optical flat with one sensor as a calibration method, the remaining stage inaccuracy will be at least $1.0 \mu\text{m}$ due to these random inaccuracies. Thermal effects do have significant influence on the measurement data. Within a temperature deviation of 0.35 K , the sensor values deviated 300 nm . If the temperature changes after calibration, it is expected to cause an offset over the whole measurement, which could be compensated for by software. If the temperature changes during

the measurement, errors will be introduced due to this temperature change which could not be compensated for. This calibration method does not require an extra sensor, but is limited to compensating for reproducible inaccuracies and is sensitive to temperature deviations during the measurement.

4.1.5 Addition of reference sensors

By adding one reference sensor to the system, the random stage inaccuracies can be compensated for partly. The reference sensor is at a distance of 0.02 m from the main sensor, as this would be required if a sample is measured. Due to the distance between the reference sensor and the main sensor, any stage inaccuracies in Rx or Ry will lead to an error in z. By measuring with one reference sensor, a distinction between the error in Z, Rx and Ry cannot be made. This could lead to an error of $3 \mu\text{m}$ since the measured roll is $150 \mu\text{rad}$ and the reference sensor is at a distance of 0.02m from the main sensor ($z = \alpha * L = 150 \mu\text{rad} * 0.02\text{m} = 3 \mu\text{m}$). The results of adding 1 reference sensor to the system, shows that the measured stage inaccuracy is reduced to $1.6 \mu\text{m}$. This suggest that part of the stage inaccuracy in z is compensating the error due to roll, which is fortunate, but not guaranteed with other stages. The position of the reference sensor with respect to the main sensor has influence on the results. The position of the sensor could be optimized by first characterize the pitch and roll of the stage, after which the optimum location could be determined. The flatness measurement with one reference sensor is an improvement in comparison with only using the main sensor, which lead to $3.3 \mu\text{m}$ deviation. The measured stage inaccuracy is still higher than just the random inaccuracies which could be compensated for when using the calibration method. Adding one sensor does therefore not result in better inaccuracy compensation in comparison with only using the main sensor with the calibration method. The results of the addition of three reference sensors to the main sensor shows that the stage inaccuracy is reduced to $0.13 \mu\text{m}$.

4.1.6 Setup limitations

The stage inaccuracy of the measurement method with three reference sensors is $0.13 \mu\text{m}$ or 130 nm . An overview of introduced error and the performance of the setup with different configurations is shown in figure 51. The remaining errors are introduced by the flatness of the optical flat ($<60 \text{ nm}$), the temperature deviation ($<50 \text{ nm}$) and due to a lower spatial resolution ($<100 \text{ nm}$) (the last will be compensated for when using three reference sensors). These three errors add up to approximately $<110 \text{ nm}$ (or $<210 \text{ nm}$ when using less than three reference sensors.) The values for temperature deviation and the spatial resolution are specific for this setup, but give an order of magnitude of the introduced errors. Additionally, the sensors are specified to have an error of 600 nm over the whole range of the sensors. Since a relatively small part of the sensors is used, the expected sensor error is $<100 \text{ nm}$. Before verifying and properly connecting the sensors, the remaining stage inaccuracy was 900 nm . It is therefore recommended to always validate the performance of the sensors if possible. To further increase the performance of the setup, several steps could be taken. Firstly, a better performing sensor could be used, which decreases the sensor error. The next boundary is the temperature deviation which is dependent on the setup and available measurement time. Only when these factors are under control and optimized, the flatness of the optical flat will be the limiting factor ($<60 \text{ nm}$). Unfortunately the flatness of the optical flat could not be verified, but is expected to be within specification. The remaining deviation of $0.13 \mu\text{m}$ is a major improvement in comparison with the random stage inaccuracy of $1.0 \mu\text{m}$. The remaining deviation could be decreased by using sensors with less errors, decreasing the influence of temperature deviations and using an optical flat with a better flatness specification. For further research it is recommended to test the setup with a main sensor with less introduced errors, since the sensor is expected to be the bottleneck in the current setup.

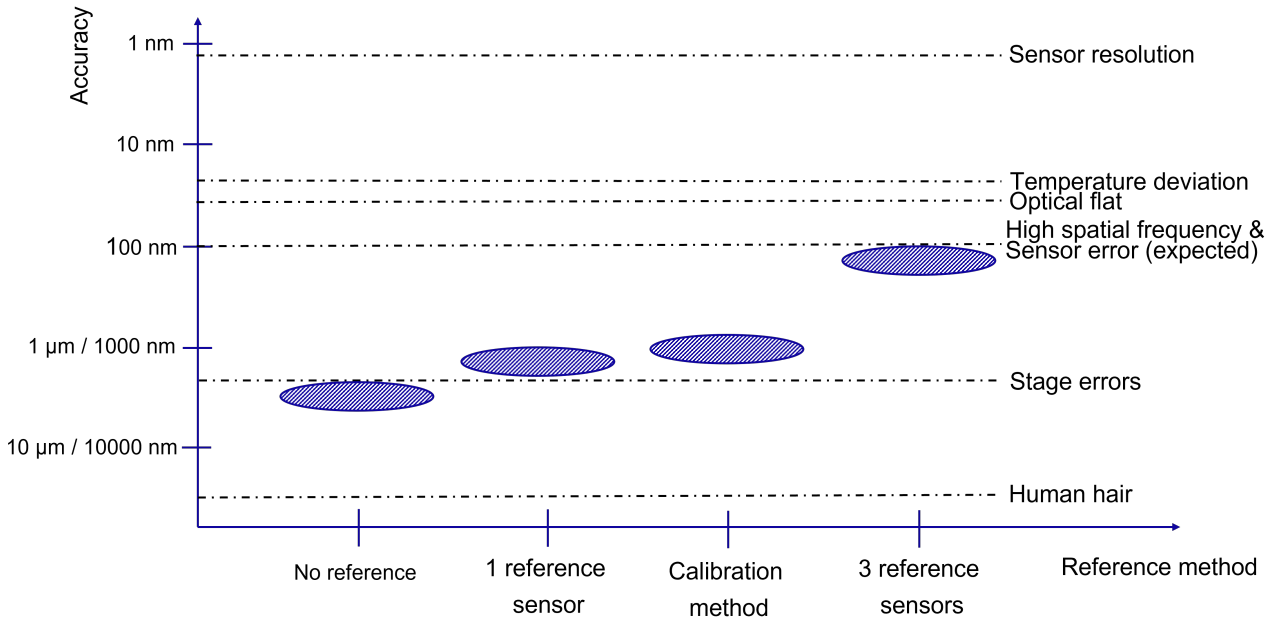


Figure 51: Setup performance and limitations

Chapter 5: Conclusion and outlook

This section contains the conclusions and the recommendations for further research (outlook).

5.1 Conclusion

The goal of this research was to fill the gap found in literature on performing point-wise flatness measurements with a higher accuracy than stage inaccuracies. This gap has been filled by determining the order of magnitude of stage inaccuracies along with the influence of these inaccuracies on point-wise flatness measurements and how to improve these. A feasibility demonstrator has been built and tested to determine flatness with a better accuracy than stage inaccuracy. To account for these stage deviations, the stages have been characterized. Stage inaccuracy consists of reproducible and random inaccuracies. Random inaccuracies are obviously more difficult to account for, since these have to be measured simultaneously when determining flatness based on point-wise measurements. Reproducible stage inaccuracies can be compensated for by measuring a known flat surface (optical flat) prior to a sample to characterize the stage. The data is stored and used to account for the reproducible part of the stage inaccuracy as a calibration method. The measurement method described in this research does not only compensate for reproducible stage inaccuracies, but also for random stage inaccuracies. The stage inaccuracies have been measured by adding either 1 or 3 reference sensors along with a main measuring sensor. During the research, the following questions are answered:

- What is the order of magnitude of the different stage inaccuracies and what is the influence in z measurements?
- What are the improvements in z measurements by calibrating the setup or adding either one or three reference sensors?
- What are the next physical limiting factors in accuracy after implementing the reference sensors?

The order of magnitude of the different stage inaccuracies is determined by measuring an optical flat on the stage. The total measured stage inaccuracies are $3.2 \mu\text{m}$, which is a combination of inaccuracies in z , R_x (pitch) and R_y (Roll). The measured inaccuracies for R_x and R_y are $85 \mu\text{rad}$ and $150 \mu\text{rad}$ respectively. The data shows that part of the inaccuracy in R_x and R_y is compensated by inaccuracy in z , which is fortunate, but not guaranteed with other stages. Although these values are specific for this setup, the values give an indication for expected stage inaccuracies with similar stages. A similar setup as described in this research could be used to characterize any linear stage.

To verify the improvement by either using reference sensors or an optical flat for calibration, the stage inaccuracies have first been characterized. Characterization of the stage is recommended for any similar setup, since reproducible inaccuracies could be compensated for without the addition of reference sensors. The stage inaccuracy have been split into a random and a reproducible inaccuracy. With the setup in this research, the inaccuracy was partly reproducible which could be compensated for with the calibration method and lead to major improvements ($1.0 \mu\text{m}$). The remaining random part could not be compensated for by the calibration method, so reference sensors have been added to the system. The addition of 1 reference sensor resulted in a remaining inaccuracy of $1.6 \mu\text{m}$. The results did improve when compared to the system without using any compensation, but did not improve in comparison with using the calibration method. For this specific setup, adding 1 reference sensor is therefore not recommended, since the calibration method performs better and does not require an additional reference sensor. The addition of 3 reference sensors did improve the results significantly, with a remaining inaccuracy of $0.13 \mu\text{m}$.

To discover the next physical limiting factors, the remaining measured stage inaccuracy is analyzed. The remaining measured stage inaccuracy is due to a combination of several limiting factors. The error introduced by the sensors is expected to be a significant part of the remaining inaccuracy. Other physical limiting factors were the introduced error by the flatness of the optical flat and ambient temperature deviations. Overall, the method of using reference sensors in order compensate for stage inaccuracies during flatness measurements is proven to work, mainly when three reference sensors are used.

5.2 Outlook

This section will describe several recommendations for further research.

5.2.1 Different sensor placement

The setup uses three reference sensors in a circular pattern of 120° to measure the stage inaccuracies z , R_x and R_y . During the research all three stage inaccuracies were measured, which required three reference sensors. However, if a different sensor placement is used, it is expected to obtain the same stage inaccuracy compensation with two reference sensors. If the sensors would be placed on one line as shown in figure 52 and figure 53, one less reference sensor is required. The orientation of the line is arbitrary, in this example the sensors are placed parallel to the y axis. The setup is not able to measure R_y , but in this configuration it is not required to be measured for stage inaccuracy compensation. So the setup is blind for R_y , but also insensitive for any deviation in R_y . Any deviation in R_y would result in the same deviation in all three sensor measurements. Since the measurement setup is based on relative measurements between the main sensor and the reference sensors, any deviation in R_y will be canceled out. This sensor configuration is recommended to be tested since the amount of sensors for full stage inaccuracy compensation is reduced from 3 to 2 sensors.

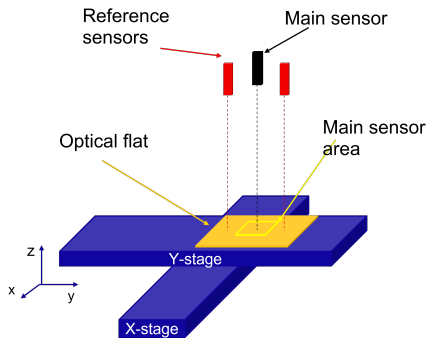


Figure 52: 2 reference sensors placement

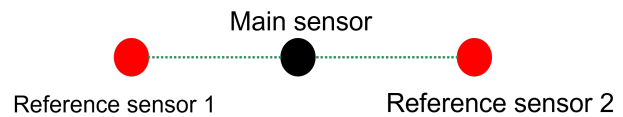


Figure 53: 2 reference sensors placement above

5.2.2 Calibration method in combination with reference sensor

During the research a calibration method is described which accounts for reproducible stage inaccuracies. The reproducible part of the stage is measured and characterized. Since part of the inaccuracy reproduces, the data of the calibration can be used to compensate for this inaccuracy. As the reproducible inaccuracy is compensated for, the remaining inaccuracy is the random inaccuracy. By combining the calibration method with the measurement system with 1 reference sensor, the measurement method could be improved. The system is physically the same in comparison with using 1 reference sensor (see Figure 54), while improvements are expected. Since the reproducible inaccuracies are accounted for by the calibration method, the remaining inaccuracy is $1.0 \mu\text{m}$. The remaining error when using 3 reference sensors is $0.13 \mu\text{m}$. The result is expected to be somewhere in between $0.13 \mu\text{m}$ and $1.0 \mu\text{m}$. It is recommended to perform a test with the combination of removing reproducible inaccuracies by calibration and using 1 reference sensor to account for a part of the random inaccuracy.

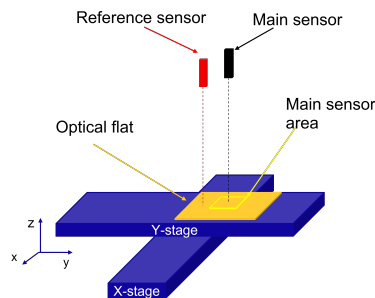


Figure 54: Sketch of research system 2: One sensor for z referencing

Chapter A: Literature report

Removed due to IP reasons

References

- [1] P. de Groot, J. Biegen, J. Clark, X. C. de Lega, and D. Grigg, “Optical interferometry for measurement of the geometric dimensions of industrial parts,” *Applied Optics*, vol. 41, 2002.
- [2] P. USA, “Stage inaccuracies definition.” [Online]. Available: <https://www.pi-usa.us/en/tech-blog/straightness-and-flatness-of-air-bearings>
- [3] R. S. Figliola and D. E. Beasley, “Theory and design for mechanical measurements, second edition,” *European Journal of Engineering Education*, vol. 20, pp. 386–387, 1 1995.